Atomic Energy of Canada Limited

LONG TERM IRRADIATION OF SAP-CLAD, UO_2 FUELLED, TREFOIL BUNDLES IN THE X-7 ORGANIC COOLED LOOP

Exp-NRX-70911

by

R.F.S. ROBERTSON, H.E. THEXTON, D.E. LEW,
R.D. MacDONALD and K.G. HEAL

Chalk River, Ontario

May, 1963

AECL-1782

LONG TERM IRRADIATION OF SAP-CLAD, UO_2 FUELLED, TREFOIL BUNDLES IN THE X-7 ORGANIC COOLED LOOP

Exp-NRX-70911

by

R. F. S. Robertson, H. E. Thexton, D. E. Lew,*
R. D. MacDonald and K. G. Heal

SYNOPSIS

An irradiation of experimental fuel bundles of UO_2 clad in Sintered Aluminium Product (SAP) sheaths was performed in the X-7 loop in the NRX Reactor from August to November 1961. The twofold objective of this irradiation was to gain confidence in the use of such a fuel in an organic coolant and to assess the fouling problem associated with a coolant which was as "clean" as the existing technology could produce.

The trefoil bundles successfully underwent an irradiation of 2400 MWD/Tonne U (max.). The maximum sheath temperature was 460°C in a coolant temperature of about 310°C. Surface heat fluxes were roughly 100 w/cm^2.

After irradiation a film of about 80 μm thickness was found covering the sheath over fuelled sections. The film was by weight 40% polymerized organic and 60% Fe_3O_4. The net effect of the film was to increase the pressure drop across the fuel by 50% and increase the sheath temperature by 60°C.

The SAP sheath showed no effects of irradiation except for small apparent increases in diameter at two out of eighteen planes measured. The appearance of the UO_2 was similar to that of UO_2 irradiated in pressurized water loops at similar heat ratings.

The stability of the fuel and the thinness of the fouling layer were encouraging indications that a successful fuel and coolant for an organic cooled reactor could be developed.

* Attached to AECL from Atomics International
Canoga Park, California

Chalk River, Ontario
June, 1963

TABLE OF CONTENTS

TABLE OF CONTENTS (Cont'd)

TABLES

FIGURES

LONG TERM IRRADIATION OF TREFOIL BUNDLES

IN X-7 LOOP

1. INTRODUCTION

The test described in this report is one in a series planned to assess the feasibility of SAP* clad-UO_2 as a fuel for organic cooled, D_2O moderated power reactors.

This test was conducted in cooperation with the Canadian General Electric Company, Peterborough, Ontario and with the USAEC. The fuel bundles were of AECL and CGE design and were manufactured by CGE in Peterborough. An Attapulgus clay column for maintaining coolant purity was provided by Atomics International, Canoga Park, California, who together with CGE also provided man-power assistance throughout the irradiation. The irradiation was performed by AECL forces in the X-7 loop in the NRX reactor.

2. OBJECTIVES

The main objective of this test was to perform a long term irradiation to demonstrate the feasibility of SAP clad, UO_2 fuel for future organic cooled power reactors. It was hoped to operate at conditions approximating those in a future power reactor. Proposed maximum conditions were:

Surface heat flux	113 w/cm^2
Coolant temperatures	
Fuel Inlet	304°C
Fuel Outlet	359°C
Sheath Temperature	450°C
$\int k d\theta$ **	44 w/cm
Average velocity of coolant past fuel	7.1 m/sec.

---

* SAP, Sintered Aluminum Product, is a mixture of Al and Al_2O_3 produced by power metallurgy techniques.

** See Section 8.2

As a result of the test it was hoped to obtain information on two important aspects of fuel and coolant technology (1)

1. The fuel under irradiation would approximate one segment of a future, larger, power reactor fuel bundle and such design features as circumferential variations in sheath temperatures, temperature variations in narrow coolant channels, and the thermal and mechanical stability of the fuel bundle would be studied.

2. The deposition of fouling films on in-reactor heat transfer surfaces is a problem in the organic cooled reactor concept. During this test it was intended to keep the coolant at as high a state of purity as was compatible with the technology at that time and to study the build-up of deposits on fuel surfaces under these conditions.

Subsidiary objectives were:-

(a) To determine whether Zircaloy-2 clad in stainless steel or aluminum picked up significant amounts of hydrogen on exposure to the high temperature organic coolant.

(b) To irradiate an inter-bundle fuel latching mechanism to assess the behaviour of this type of mechanism in organic liquid at high temperature.

The results of these two parts of the experiment will not be discussed in this report, but may be found in references (5) and (6).

3. PREPARATION OF FUEL BUNDLES

Fuel bundles were prepared by CGE at Peterborough, Ontario.

Two trefoil bundles, each containing three SAP clad fuel elements approximately 61 cm long were prepared. A dummy trefoil bundle containing a prototype inter-bundle latch and corrosion specimens was also fabricated. An outline of the construction of the bundles is given below, full details including all measurements, etc., can be found in references (2) and (3). In this report each rod 61 cm long containing the UO_2 fuel will be referred to as an element and the combination of three elements will be referred to as a bundle. The assembly of bundles forms a fuel string.

3.1 The Fuel Element

3.1.1 The UO_2 Pellets

UO_2 powder with an enrichment of 4.411 wt % U-235 in total uranium was pressed into pellets and sintered by conventional techniques. Average dimensions of pellets are given below; full dimensions may be found in (2).

Average UO_2 Pellet Data

Enrichment	4.411 w/o U-235 in total U.
Length	1.98 cm
Diameter	1.415 $\pm$ 0.0025 cm
Density	10.50 g/cm^3

Pellets were dished at one end to a depth of 0.5 mm and were stacked in groups of 30 in lengths of 57.7 cm. Cutting of pellets was performed where necessary. Circumferential grooves (0.76 mm wide x 1.3 mm deep) for flux monitors were cut in the central pellet of each stack. Flux monitors were wires of 0.71 mm diameter made from Cu - 0.568 wt % Co alloy.

3.1.2 SAP Sheaths*

Sheaths were made from SAP M583 extruded finned tubing. The SAP M583 billet which contained nominally 7 wt % Al_2O_3 was obtained from AIAG, Switzerland and the tubes were made by General Impact Extrusions Limited, Toronto, Ontario. Extrusion temperature was 427° C.

The six fins which were each 1 mm high were spaced equidistantly around the circumference of the tube and spiralled down the tube such that they made one revolution each 91 cm (36 inches). Tubes with left and right hand spirals were made. Each bundle contained one element with a left hand spiral, one with a right hand spiral and one with the fins machined

---

* The designations and origins of the various SAP materials are discussed by Boxall in reference 4.

off from 130° of peripheral surface (See Figure 1). The reason for removing some fins was that the elements were to be assembled into a bundle with fin-on-sheath geometry and to provide this, parts of some fins had to be removed from one element in each bundle.

The tubes were nominally 1.57 cm OD and 0.7 mm wall thickness. The overall length, including end plugs was 61 cm. End plugs were made from M257 SAP.

Slots were milled in specified fins to carry thermocouples. These slots were 0.5 mm wide by about 0.8 mm deep. At the end of each slot a hole 0.5 mm in diameter was drilled a further 4 mm into the rib to house the end of the thermocouple.

Fins on all tubes were also machined off to a distance of 4 cm from each end; this was necessary to allow the swaging and hot bonding of end closures.

3.1.3 Assembly of the Element

One end closure was made by a swaging technique, the fuel was loaded into the tubes, the annular gap was evacuated and refilled with He and the other end plug was swaged on. The seals were hot bonded by immersing them for 20 minutes in a lead bath at 600° C. The elements were then machined to size. Typical elements are shown in Figure 1.

3.1.4 Inspection and Testing of Element

Each seal was radiographed and then the elements were helium leak tested by holding them in a glass tube evacuated to a pressure of one to two microns Hg for 10 minutes. The He leak detector was calibrated to detect a leak of 8×10^{-7} atm-cc/sec. No indications of any leak were found.

Elements were then cycled in a He atmosphere from room temperature to 480° C for one hour and then to room temperature. Three such cycles were performed followed by a further He leak test which also gave negative results.

Finally, complete dimensional measurements were made on each element. The table below shows typical nominal dimensional data. Full data for each element are given in reference 2.

Typical Element Measurements

Fuel	Stack length	57.7 cm
	Stack weight	950 g.
Sheath	OD	1.57 cm
	ID	1.43 cm
	Thickness	0.07 cm
Clearance	Axial	0.74 cm
	Diametral	0.10 - 0.15 mm

3.2 The Fuel Bundle

3.2.1 Thermocouples

Twelve thermocouples were located in the fins of the six elements. These thermocouples were of the sheathed variety with the chromel-alumel conductors embedded in MgO insulant and sheathed in stainless steel sheaths 0.51 mm in diameter. The measuring junction was embedded in the fin and the wire ran the length of the fin embedded in the groove. About 1 metre from the hot junction a transition was made from 0.51 mm to sturdier 1.0 mm diameter thermocouple wire. Details of how the thermocouple were attached and of the transition junctions are given in reference 3.

3.2.2 Assembly and Designation

Three elements were assembled into a fuel bundle. They were joined at each end by special plates made from type 304 stainless steel.

Specially shaped filler pieces, made of 65 S aluminium and sized to decrease the amount of coolant associated with the bundle and hence to give the desired coolant flow rate were added to the bundle. Grooves ran along the outer, curved, surface of the filler pieces to act as channels for thermocouple wires and for the "bird cage" wires which held the bundles together to form the fuel string.

The elements were mounted such that separation between sheaths was maintained by fin-on-sheath geometry. The closest approach of any two elements was 1 mm. Figures 1-3 show different stages in the assembly of a bundle.

Two bundles were irradiated. Bundle DEA contained elements DEB, DEC and DED while bundle DEE contained elements DEF, DEH and DEJ. This is illustrated in Figure 4 which also shows the location of the various sheath thermocouples.

A finished bundle was 61.8 cm long and weighed 3.5 kg. The outside diameter of the bundle was such that a 3.7656 cm diameter ring gauge could pass over it without undue force being exerted.

3.3 The Fuel String

3.3.1 Addition of Thermocouples

Thermocouples to measure bulk coolant temperature were next added to the bundles. These thermocouples were similar to those on the sheath except that they were made from 1.0 mm diameter sheath throughout. They were attached to the bundles by drilling 1.02 mm diameter holes through the end plates and filler pieces in the appropriate positions, force fitting the thermocouples through the holes and peening the edges of the holes to lock the thermocouples in place. The ends of the thermocouples were bent to locate the hot junctions in the desired positions, that is, 1.25 to 2.50 mm from any part of the fuel assembly. The thermocouple leads were laid into the slots in the filler pieces and fixed into place by laying a larger diameter wire over them and peening the edges of the slot to hold that wire in place.

3.3.2 Assembly

The two bundles were now mounted one above the other with DEA on top. The dummy fuel bundle containing the prototype latching mechanism and the corrosion specimens (1) was mounted above DEA. All three bundles were held together by the "bird cage" type of carriage which has been used for other irradiations at AECL. Essentially the bundles were held together by wires in tension which ran down the grooves in the filler pieces. These wires were fixed by carriage pieces above and below the fuel string. The wires were kept in tension by a latch and a spring in the upper carriage and tension could be increased by tightening nuts at the top of the assembly. The spring was sized such that even when the bundle was at operating temperature, the carriage wires would still be in tension. Sufficient tension was applied initially to prevent excessive movement of the bundles one relative to the other. The filler pieces of adjacent bundles interlocked to give some further rigidity to the assembly and to prevent relative rotation of the bundles.

Manufacture of the fuel string to this stage, which was carried out by CGE at Peterborough, Ontario, also included addition of the hanger bar.

The fuel string was now carefully crated and shipped to Chalk River.

On arrival at Chalk River the fuel string was uncrated, hung in a vertical position in NRX and was visually examined thoroughly. The tension on the individual carriage wires was adjusted to make the assembly hang true and the nuts were locked to prevent their being loosened by vibration. The Unibolt cap, which would close off the test section of the X-7 loop, was connected to the hanger bar.

The thermocouple leads were then sealed through the "Conax" type gland seal on the Unibolt cap and the extension leads were connected to the thermocouple cables by the usual "potting" type of connection (7).

Just prior to installation the assembly was washed off with acetone and allowed to dry.

4. THE X-7 LOOP

4.1 General Description

The X-7 loop (8) is a facility in which an organic liquid can be recirculated at temperatures up to 427°C and pressures up to 21 kg/cm^2 past an experimental fuel assembly held in the core of the NRX reactor. The flow rate of coolant may be as high as 130 ℓ/min.

Immersion or induction heaters provide 80 kw of heat in addition to the nuclear heat from the fuel. The loop coolers, in a parallel circuit to the main circuit, can remove 200 kw of heat . A second parallel circuit contains the loop filters and adsorption column which will be discussed more fully in Section 4.4.2. In a third circuit, a flow of coolant from the lowest temperature point in the system, just after the loop coolers, is maintained to the vapour phase of the surge tank to act as a degassing circuit.

4.2 The Test Section

The test section of the loop consists of a stainless steel pressure tube of 3.57 cm ID and 0.125 cm thick. This tube, which is inserted in a fuel rod position of the NRX reactor, contains the fuel bundles under irradiation. The coolant is circulated upwards through the stainless steel tube from the bottom; Figure 5 shows a schematic representation. The coolant entrance and exit are connected to the organic circulating system by welded carbon steel piping. The top closure of the tube is made by a "Unibolt" closure adapted so that thermocouple leads can be taken out through a modified Conax seal.

Heat losses from the stainless steel tube are minimized by larger diameter Al tubes around the steel tube making annuli which contain stagnant Argon or flowing air.

4.3 The Coolant

4.3.1 Chemical Composition

The coolant used in the X-7 loop was a mixture consisting of principally ortho- and meta- terphenyl with the addition of high boiling tars (HB), obtained from the OMRE reactor, NRTS, Idaho. At the start of the irradiation, a typical composition was:-

o- terphenyl	38 wt %
m- terphenyl	22 wt %
p- terphenyl	2 wt %
biphenyl	5 wt %
HB	30 wt %
Unaccounted	3 wt %

This mixture was sufficiently fluid that it could be pumped through the loop at room temperature. The only trace heating on the loop was on stagnant lines leading to pressure or flow measuring instrumentation or in lines in which a vapour phase would be present.

4.3.2 Purity Specification

Work by AI on OMRE* had shown that to minimize fouling on fuel surfaces, the ash content of the coolant and the PCFT number should be low.

The PCFT (Pyrolytic Capsule Fouling Test) is a rather arbitrary test which involves heating 240 g of the coolant for 24 hours in a stainless steel capsule under nitrogen at 700 psi (49 kg/cm^2) at a bulk temperature of 316°C. (9). The capsule contains an electrically heated

---

* OMRE is the Organic Moderated Reactor Experiment operated at the National Reactor Testing Station, Idaho by Atomics International for the USAEC.

tube which is kept at 566°C, as measured by a thermocouple inside the tube. At the end of 24 hours heating the deposit on the tube is weighed and the weight of this deposit, in milligrams, is the PCFT number.

During this test it was hoped to maintain the following conditions:-

Ash	< 10 ppm
PCFT	< 15 mg.

Previous tests had indicated that in the X-7 loop the ash specification could be adequately met by the use of sintered stainless filters of 5 μm nominal pore size in a by pass circuit. PCFT numbers however had been as high as 100 mg. Consequently some means of reducing the PCFT number was required. AI had had some success using columns filled with Attapulgus clay as adsorbent beds and it was decided to try this method for the present test. A column was designed and fabricated by AI and was shipped to AECL.

4.4 The Coolant Purification Circuit

4.4.1 The Clay Bed

The clay, Attapulgus clay of 30-60 mesh, was held in a stainless steel can 53 cm in diameter and 61 cm high, which was open at the top and closed at the bottom except for a centrally located inlet tube. This can held about 80 kg of clay. The bottom of the can was first lined with a pad of Pyrex glass wool, the clay was then poured in until the can was almost full and then another pad of Pyrex glass wool covered the top above which was placed a screen of woven stainless steel wire. This assembly was held inside a large vessel roughly 75 cm in diameter and 1 metre high. The entrance tube for the organic coolant was welded through the dome shaped bottom of the vessel and ended in a cone shaped receptacle. A spigot, with the lower end rounded, was welded on the tube leading into the bottom of the can holding the clay. The spigot fitted into the cone shaped receptacle and was held as a press fit by the weight of the can plus clay. This is sketched diagramatically in Figure 6.

The top of the vessel was closed by a large blind flange. A soft iron gasket was used.

The coolant exit tube left the vessel near the top. There was also a centrally located thermocouple to measure the temperature of the clay bed.

4.4.2 Design Conditions for Clay Bed

A clay bed of this type operates most efficiently at an elevated temperature, above 300°C if possible (10). Since the designed flow rate of coolant up through the bed was only about 340 ml/min, even though it entered at high temperature, heat losses would be large and extra heating would be necessary to maintain the bed at high temperature. Hence piping was wound around the outside of the vessel through which a flow of 3-1/2 ℓ/min of loop coolant could pass. It was hoped that this would keep the vessel at a sufficiently high temperature but experience soon proved that extra heat had to be added.

4.4.3 The Clean-up Circuit

Figure 6 shows a schematic representation of the clean-up circuit. The pump, a Milton-Roy diaphragm metering pump maintained a flow of 340 ml/min of loop coolant through the clay bed. Another flow of 3.5 ℓ/min, provided the extra heat to the clay bed. This large flow left and re-entered the main circulating system such that the main loop circulating pump head provided the driving force for coolant flow. This flow also lead to the loop filters. Hereafter the flow of 340 ml/min to the bed will be referred as the feed flow and the flow of 3-1/2 ℓ/min which heated the column will be referred to as the heating flow.

Initially, strap on heaters were used to provide heat to the feed and heating flow, 2-1/2 kw being provided for the feed and 12 kw for the heating flow. This type of heating gave continual trouble in that temperature control was difficult and overheating occurred leading to coking and polymerization of the coolant in the small diameter piping. Consequently a 15 kw immersion heater was finally put in the heating flow. The feed flow piping was wound around the outside of the heater vessel under the lagging to increase the temperature of the feed flow. This arrangement performed with no further difficulty.

The filters were those used in previous tests and were of sintered stainless steel. Two filters, one of which was in operation, were mounted in parallel. Filter pore size could be varied from a nominal 40 μm to a nominal 5 μm.

The sampling system was in this circuit and was arranged such that samples of the coolant could be taken before it entered and after it left the column.

5. LOG OF EVENTS

This section gives in brief narrative form a description of the more important events involved in the in-reactor irradiation, and the sub-

sequent fuel removal and examination.

5.1 Loop Operation Prior to Installation of Fuel (June 26 - Aug. 15)

The test prior to this one, the "Fouling Test"(11), was completed on June 26th, 1961. From then until August 14th, the test section of the loop remained in-reactor with coolant recirculated through it but with no fuel present. It was during this period that the new clay column was added to the loop and circulation through it commenced.

During the Fouling Test, and during previous tests, the Fe content of the coolant varied between 3 and 8 ppm, averaging about 4 ppm, while the PCFT values were high, in the range 60-124 mg with an average about 90 mg.

The clay column was started on stream on July 14th. Flow through it was 20 ℓ/hr and the maximum bed temperature was 230°C. Operation was erratic in that during some periods flow was shut off to repair pre-heaters and during others the column operated with no pre-heat and a bed temperature of below 200°C. Nevertheless by August 1st, PCFT values had fallen to 15-30 mg and the Fe content of the coolant was at the 2-4 ppm level.

An arbitrary decision was made to renew the clay bed and on August 7th a fresh bed of clay was charged to the column and operation started again. The new bed was also subject to erratic operation and did not show any further significant reduction in PCFT values which remained in the range 15-40 mg. These values were higher than hoped for (Section 4.3.2) but, since it was not known at that time whether PCFT values and fouling were definitely inter-related, an arbitrary decision was made to start the fuel test.

5.2 Start of Fuel Test

On August 14th, 1961 the reactor was shutdown, the loop was cooled and the fuel stringer was lowered into the test section. The top closure was sealed and thermocouple leads attached to the recording instrumentation. During the insertion of the fuel string normal precautions of exclusion of oxygen and thorough flushing with N_2 were observed. The loop coolant was then brought to a temperature of about 200°C and at 0258 hours on August 15th, the NRX reactor was brought to 20 MW power. The fuel power output was calculated from a knowledge of the flow rate of the coolant, the temperature at the inlet to the fuel and the temperature rise across the fuel. The reactor power was then raised in successive 5 MW stages, the above calculation being repeated at each stage. It was apparent that the fuel string would produce over 220 KW at full reactor power, significantly above the

design figure of 175 KW. During a reactor trip early on August 15th, the fuel in NRX was reshuffled and on a subsequent start-up the power output from the fuel string was found to be 170 KW at 40 MW reactor power.

5.3 Period August 15th - 23rd

During this period operation was rather erratic. The coolant temperature at the fuel inlet was about 230°C for most of the period except for a period of about 57 hours when it was about 280°C. The temperature rise across the fuel was 50-53°C. Sheath temperatures during this period were not known because of instrumentation difficulties.

Flow was not started to the clay column until August 18th and throughout the period there was no pre-heat to the column feed. At the start of the period of elevated coolant inlet temperature the bed temperature was about 250°C but it fell steadily over a few days to a steady level of about 170°C. PCFT values in the coolant were 20-30 mg with one high value of 50 mg (See Figure 7).

On August 21st, NRX shutdown for the regular monthly maintenance period. During this time the loop coolant was reduced to a temperature of about 200°C until the reactor started up again on August 23rd. During this shutdown the instrumentation associated with the sheath thermocouples was brought into working order.

5.4 Period August 24th - September 13th

On reactor start-up the coolant inlet temperature was kept at 240°C for a few days. All sheath thermocouples showed temperatures rather higher than calculated but thermocouple No. 4 showed the largest discrepancy. It indicated a temperature of 385°C, some 40°C higher than anticipated. On September 1st, the coolant temperature was increased. At an inlet temperature of 310°C thermocouple No. 4 showed a temperature of 435°C, only about 25°C higher than expected. However on September 4th, the reading of thermocouple No. 4 abruptly increased to 446°C for no change in coolant temperature. Thermocouples Nos. 10 and 11 showed similar abrupt changes while the others did not. This phenomenon is dealt with more fully in Section 7.2.4. In general throughout the test, thermocouple No. 4 showed the highest temperature, usually 10 to 20°C above the other thermocouples.

To ensure that the maximum sheath temperature did not rise above the design figure of 450°C, the coolant inlet temperature was gradually lowered from 310°C to 288°C.

On August 29th, the strap on heaters to the heating and feed flows to the clay column were replaced by an immersion heater. From this time

on no difficulties were observed with the operation of the column. The bed temperature was still not as high as desired but generally operated at a temperature of 250-280°C. Concurrent with the better operation of the column, the PCFT values of the coolant fell to generally less than 10 mg.

Operation of the loop was interrupted by one incident on August 25th when the reactor had to be shutdown, the loop cooled and the main control valve in the loop replaced. This necessitated draining part of the loop piping and cutting and rewelding operations. During this period care was taken to flush as thoroughly as possible with N_2 before refilling the affected part of the circuit with coolant. The total operation took about 10 hours.

During this period the first indications appeared that the pressure drop across the fuel bundle was increasing.

On September 13th the reactor was shutdown to service another loop. During the shutdown some fuel shuffling took place in the reactor core.

5.5 Period September 13th - September 22nd

Late on September 13th the reactor was started up and during the start up, experiments described more fully in Section 6.2.6, were performed to determine whether the high temperature observed on thermocouple No. 4 was caused by bowing of the fuel bundle with consequent starvation of coolant in the region of the thermocouple. Results indicated that bowing was negligible.

During the remainder of this period when the coolant temperature at the fuel inlet was 288°C, thermocouple No. 4 showed a temperature of about 446°C.

The PCFT values in the coolant showed an increase from around 10 mg to 20-40 mg. This increase may be associated with a leak of a fluid known as HB-40 into the loop coolant. This is discussed more fully in the next section.

On September 18th the reactor was shutdown for the regular monthly maintenance period.

5.6 Period September 22nd - October 27th

Prior to start up it was decided to limit the temperature of the coolant at the inlet to the fuel such that the maximum sheath temperature indicated by any thermocouple should not be greater than 465°C.

There was actually an estimated 10°C temperature difference between that of the sheath and that at the fin. Hence the actual maximum temperature of the sheath was limited to ~475°C.

This period started off with a coolant inlet temperature of 304°C. This was subsequently lowered to 288°C to keep the indication from thermocouple No. 4 within prescribed limits. The maximum temperature read by this thermocouple was 452°C, indicating a maximum sheath temperature of 460°C.

On September 27th the flow to the clay columns was stopped to repair a cracked diaphragm in the metering pump. This diaphragm is actuated by a piston forcing HB-40* liquid against it. Actually this diaphragm may have been cracked as early as August 28th and HB-40 may have been forced into the loop from that time on. However up to about September 25th the loss rate of HB-40 from the pump averaged about 1 litre per day. However by September 25th the loss rate had increased to 200 ml/hr and on September 26th when it was repaired, the loss rate was 400 ml/hr. It is estimated that a maximum of 50 kg of HB-40 was injected into the loop (See Section 6.3.1).

The PCFT values for the loop coolant decreased during this period to values generally below 5 mg.

The pressure drop across the fuel string showed a very significant increase between September 22nd and October 7th.

On October 23rd the scheduled monthly shutdown of NRX took place.

5.7 Period October 27th - November 20th

Operation during this period proceeded relatively smoothly. Coolant inlet temperature was gradually lowered from 287°C to 283°C and the temperature indicated by thermocouple No. 4 fell from 463°C to 456°C as the coolant temperature was lowered.

PCFT values were generally 5 mg or less with a few values around 10 mg.

The pressure drop across the fuel showed a slight increase.

On November 20th NRX shutdown for the scheduled monthly shutdown.

---

* HB-40 is the trade name of a fluid marketed by the Monsanto Chemical Company. It is a mixture of partially hydrogenated o-, m- and p-terphenyl.

5.8 Fuel Removal and Examination

After reactor shutdown, the coolant temperature was lowered to below 200°C but was kept circulating for 41 3/4 hours. Coolant flow was then stopped, the loop was depressurized, the test section closure was opened and the fuel string was withdrawn into the large shielded flask. During this time the fuel was cooled in a stream of nitrogen which flowed past it at a rate of 11-23 m^3/hr. With the cooling flow of N_2 still on, the fuel stringer was transported by the flask to the vertical storage block in the NRX building and was lowered into a long aluminium tube full of HB-40. During all this period the sheath thermocouples were connected to instrumentation and during the entire transfer procedure the fuel sheath temperature did not exceed 182°C.

The stringer was left standing in the HB-40 until January 15, 1962, a period of 54 days. It was then removed, in air, to the examination cell in a 25 ton transfer flask. In the examination cell the sheath temperature was found to be not over 60°C and was actually 10-20°C lower in temperature than had been estimated (1).

In the cell the fuel was washed and a complete visual and dimensional examination took place. A fouling film of maximum thickness 80 μm was found. The bundles were dis-assembled and examination of thermocouples and dimensional checks were made.

Individual elements were transported to the Metallurgy examination cells where puncture tests to measure build up of fission product gases inside the sheaths were made. Then selected elements were cross-sectioned and polished and the fuel and the fouling film were examined in some detail.

6. RESULTS

6.1 Loop Operating Data

The various flows, velocities etc., pertinent to the operation of the X-7 loop are shown below. In all cases the variable specified was held as closely as possible to the value indicated - usually within two or three percent of the value. Where a range is given, most of the operation was at the upper limit but for one reason or another, sometimes operated within the range shown.

LOOP OPERATING DATA

Flow rate to test section	96 ℓ/min.
Average velocity in test section	7.1 m/sec.
Absolute pressure at inlet to fuel	21.1 kg/cm^2
Flow to Surge Tank	2.3 ℓ/min.
Flow to Filters	2 - 4 ℓ/min.
Flow to Clay Columns	0.34 ℓ/min.

6.2 Fuel Operating Data

6.2.1 Summary

Table 1 shows maximum conditions in each of the periods outlined. The proposed conditions are also given for comparison. The various parameters outlined are dealt with in more detail in the sections below.

6.2.2 NRX Power

Figure 7 shows a plot of NRX power as a function of time.

Reactor megawatt days for the various periods of operation were:-

August 15th - September 13th	928.0
September 13th - September 18th	173.9
September 22nd - October 23rd	1092.8
October 27th - November 20th	892.8
	3087.5 Mwd

6.2.3 Fuel Power

During each period the power output was calculated knowing the coolant flow rate, the coolant temperature at the fuel inlet and the temperature

rise across the fuel. A correction was applied for heat losses in the test section. The overall accuracy of the power as measured by this means is no better than $\pm$ 10%. Within these limits the fuel power stayed constant during any one given period as shown in Table 1. This table indicates that the fuel power decreased as the irradiation continued. This effect is fortuitous and is due to the varying fuel load in NRX during each cycle and not to any burn-up effect. To illustrate this the "f - factors" for the X-7 position during the various periods are listed below. An "f - factor" is defined as the fraction of reactor power which would be produced by a normal uranium fuel rod in the position occupied by the X-7 loop test section. It really represents the extent to which surrounding neighbours affect the power output of a given position.

	f - factor
August 15th - September 13th	0.0070
September 13th - September 18th	0.0065
September 22nd - October 23rd	0.0061_5
October 27th - November 20th	0.0063_5

The fuel string powers and total burn-up listed in Table 1 are those determined by calorimetry. The calorimetric results agreed well with burn-up calculated from chemical analysis of the fuel for Cs 137 and Pu 239 + Pu 240 after the irradiation. This is more fully discussed in Section 6.4.6.

The data for surface heat flux, $\int \kappa d\theta$ and burn-up shown in Table 1 may be calculated directly from the values of fuel power which are shown. The overall accuracy in any of these figures is no better than $\pm$ 10%.

6.2.4 Temperatures

Figure 7 shows temperature data.

The representation is somewhat formalized in that short term fluctuations are not shown and long periods during the reactor shut-down are omitted.

The temperatures plotted are:-

- Coolant temperature at inlet to fuel

- Thermocouple No. 4

- The average of the readings of thermocouples 1, 2. 3 and 6.

- The average of the readings of thermocouples 10 and 11.

The averaged readings rather than the readings of the individual couples are shown for clarity. In neither group did the reading of an individual thermocouple differ from the average by more than 10°C. Complete readings of all thermocouples will be kept on file by Fuel Development Branch, AECL. Other thermocouples listed in Figure 4 are not shown in this plot because for one reason or another they failed during irradiation.

The readings of thermocouple No. 4 are plotted since they consistently indicated the highest temperature during the irradiation. In addition, this thermocouple was the only one which indicated the sheath temperature in a sub-channel between an element of bundle DEA and the wall of the pressure tube (Figure 4). The averaged readings of thermocouples 10 and 11 indicate sheath temperature conditions for similar channels on the lower element DEE. Thermocouples 1, 2, 3 and 6 were all on sheaths facing inner channels on the top bundle DEA while DEE had no such sheath thermocouples.

Qualitative examination shows that the coolant temperature at the inlet to the fuel had to be dropped throughout the irradiation from 310°C to 283°C in order that the highest recorded sheath temperature should not exceed 460°C. The major effect occurred before October 6th and subsequent to that date inlet or sheath temperatures did not vary greatly. This will be discussed more fully in Section 7.1.

6.2.5 Pressure Drop Across Fuel

The change in the pressure drop across the fuel as the irradiation proceeded is recorded in Figure 7. The data were taken from the chart of the differential pressure recorder which measured the differential between the inlet and outlet pressures to the fuel. There was a scatter in daily readings of $\pm$ 0.15 kg/cm^2. The data points plotted represent an average reading for that day. Only periods during which the inlet temperature was 240°C or higher have been included. No temperature correction has been attempted since any correction is small and will lie within the experimental scatter.

The initial Δp (< 3 kg/cm^2) was significantly lower than the expected value of 5.5 kg/cm^2. The reason for this discrepancy is discussed in Section 7.1.

There were two main periods during which the Δp increased steeply, August 26-30 and Sept. 22 - Oct. 6. It is interesting that both these

periods occur after scheduled reactor shut-down periods, during which time the loop coolant was reduced in temperature to below 200°C. During the second, longer, period of Δp rise there were also two rather lengthy reactor shut-downs and many shorter periods. During the remainder of the irradiation the Δp did not change or only rose very slowly. Throughout the irradiation the Δp increased from $\sim$2.8 kg/cm^2 to 4.1 kg/cm^2, i.e., a 50% increase, most of which occurred before October 6th, 1961.

6.2.6 Special Experiment to Assess Bowing

This experiment, which was performed during the reactor start-up of September 13th (Section 5.5), was designed to indicate whether the abnormally high sheath temperatures (especially that of thermocouple No. 4) could be attributed to bowing of the elements at full reactor power. It was reasoned that if bowing did occur, the sub-channel between the fuel sheath and the pressure tube wall would narrow; hence the coolant velocity in that sub-channel would decrease. The net result would be a higher sheath temperature than normal because of the increased coolant temperature in the sub-channel and because of the lower heat transfer coefficient caused by the lower coolant flow rate. Furthermore, bowing would probably occur only when the fuel power output was high and uneven temperature distributions and stresses occurred.

If ΔT_f is the difference between the coolant temperature (T_c) and the sheath temperature, then $\Delta T_f = q''/h$ where q'' is the surface heat flux and h is the sheath to coolant heat transfer coefficient. If no bowing occurs, as the reactor power increases a plot of ΔT_f vs q'' should be linear, whereas if bowing does occur, ΔT_f should increase at a greater than linear rate as q'' increases.

During the start-up of September 13th, the reactor power was increased by roughly 10 MW increments and was held at each increment for a sufficient length of time for temperatures to come to equilibrium. At each power level the coolant flow was measured as were coolant inlet and outlet temperatures and sheath temperatures. Thermocouple No. 4 was taken as the reference thermocouple and its output was measured with a potentimeter using an ice bath as reference junction. The outputs of the thermocouples measuring inlet and outlet temperature were also measured in this way.

At each power level the value of q'', at the elevation of t/c No. 4 was calculated from the calorimetric data, together with the thermal neutron flux pattern given in reference 12.

T_c was calculated at the elevation of thermocouple No. 4 by assuming that the coolant temperature at that elevation was the inlet

temperature plus the proportion of the temperature rise across the fuel corresponding to the ratio of the distance of t/c No. 4 from the bottom of the fuel to the total length of the fuel.

During the experiment, the inlet temperature was decreased as power increased such that T_c should stay reasonably constant and hence, assuming no bowing, h should also be constant. Table 2 shows that the calculated value of T_c did not vary by more than $\pm$ 3°C.

T_{sh} was not corrected for any fin effect. The results are tabulated in Table 2 and plotted in Figure 8. Except for the two points at highest power, ΔT_f shows a linear dependence on q''. The straight line shown is a least squares fit of the first five points. The 95% confidence limits calculated from this are also shown.

The results thus indicate that there is a greater than 95% probability that bowing of the element to which t/c No. 4 was attached did not occur during this particular experiment. This does not mean that bowing could not have occurred during other periods of operation. Erratic temperature indications of the sheath thermocouples will be discussed more fully in Section 7.2.

6.3 Chemical Data

6.3.1 Isomeric Composition

Table 3 shows the isomeric composition of the coolant at various stages in the irradiation. Analyses for biphenyl and o-, m- and p- terphenyl were performed by conventional gas phase chromatography (13). On a given date the results shown are the average of at least two analyses. These results are believed accurate to $\pm$ 5% of the weight percentage shown.

The column headed "HB" represents the weight of High Boiling Residue as determined by the micro distillation technique (28). This is representative of all compounds with a boiling point higher than that of p-terphenyl.

The column headed " 100 - Σ" represents the difference between 100% and the sum of biphenyl and the three terphenyl weight percentages. It represents the HB fraction and any other low or intermediate boiling fraction.

The relative amounts of biphenyl and the three terphenyls did not vary significantly through the irradiation. This is to be expected in view of the very small amount of coolant under irradiation at one time relative to the total amount in the loop (a ratio of roughly 1 : 400). It is interesting to note however that after 5 Sept. the amounts of terphenyls decreased and

the " 100 - Σ" figure became significantly larger than the "HB" figure. This is probably due to the in leakage of the fluid in HB-40 from the diaphragm pump (Section 5.6). HB-40 would distill over before the HB and hence the HB figure would remain relatively constant, as it did. The "100 - Σ" figure should increase since HB-40 would be present in the sample for analysis but would not contribute to the biphenyl or terphenyl peaks on the gas chromatograph. Through the irradiation the HB averaged 30 weight % while after 5 Sept. the " 100 - Σ" rose to a steady value of about 40 weight %. Assuming that the 10 weight % discrepancy was due to HB-40 and that the loop held a total of 500 kg of coolant it can be seen that roughly 50 kg HB-40 leaked in through the defective pump diaphragm.

6.3.2 Density, Viscosity, Vapour Pressure

Table 4 shows results of density, viscosity and vapour pressure measurements made on coolant samples. All measurements were made by conventional techniques (29) (30).

Results indicate that none of these parameters varied significantly through the irradiation and were not very different from similar results obtained previously.

6.3.3 Pyrolytic Capsule Fouling Test (PCFT)

PCFT numbers were obtained regularly on the loop coolant. The method and apparatus used were precisely similar to the AI method (9).

The results are plotted in Figure 7 and recorded in Table 5.

At the beginning of the irradiation PCFT numbers were high, although a significant lowering had been achieved by the use of the clay column. It was not until the clay column could be operated at a reasonably high bed temperature that PCFT values fell regularly at 10 mg or below. The reason for the higher levels between Sept. 14 - 27 is not known but may be due to the in-leakage of HB-40 to the loop coolant.

6.3.4 Ash and Fe Concentrations

The Fe concentration in the coolant was determined routinely by X-ray fluorescence analyses (32). Results are listed in Table 5.

The lower limit of detection of Fe by this method was ~ 2 ppm during this period. (Note : This method has now been refined to the extent that the lower limit of detection of Fe is 0.5 ppm).

Ash analyses were not performed during this period. Other tests (31) have shown that the main constituent of the ash was γ-Fe_2O_3

(or Fe_3O_4) and that ash determinations agreed well with Fe determinations.

6.3.5 Water and Chlorine

Water analyses were performed by the modified Karl-Fischer method. Since results obtained during this period are now suspected of being consistently high, no detailed results are given. Analyses indicated ~200 ppm H_2O present up to the beginning of September and from then the H_2O concentration gradually fell to an indicated 100 ppm by the end of the irradiation.

At this period the presence of chlorine was not suspected as being a possible contributor to fouling mechanisms and unfortunately no analyses of the coolant were made for chlorine.

6.3.6 Dissolved Gases

Analyses for dissolved gases were performed by conventional methods. Table 6 shows some results. Only those analyses are recorded for which the reactor and the loop had been operating under constant conditions for 24 hours or more.

Dissolved O_2 concentrations were normally < 0.2 cc(STP)/kg.

The column headed "HC" denotes hydrocarbon gases which are condensed at liquid nitrogen temperatures but are not condensed by dry ice at a pressure of 10^{-3} mm Hg. This fraction probably consists of the C_2 gases and perhaps some C_3.

There was a steady flow of about 2.3 ℓ/min. from the effluent of the loop heat exchanger (the lowest temperature point in the loop) to the surge tank. The N_2 used as pressurizing gas rapidly equilibrated throughout the loop, hence the high N_2 concentrations. It is not known how fast the other gases came to equilibrium with the surge tank vapour, but it is possible that there was continued stripping to the vapour phase of the surge tank and because of the large vapour volume and because of small losses by leakage of N_2 from the surge tank, the partial pressure of any gas, except N_2, was very small. If this was so, then steady state concentrations of gases would occur in the coolant in relatively short periods of time.

The trend is apparent here which has been noticed before, that at higher coolant temperatures the amounts of H_2, CH_4 and "HC" are higher, indicating that a small amount of decomposition is taking place.

6.3.7 Radioactivities

Radioactivities in the loop coolant were generally low through-

out the test. Table 7 shows counting rates of samples counted on a β-proportional counter one hour after sampling. The results indicate a gradual decrease in the radioactivity of the coolant as the irradiation proceeded.

γ-ray spectra were taken on samples of coolant from time to time on a 100 channel pulse height analyzer. The main longer lived nuclides found present were Mn-56 ($t_{1/2}$ 2.58 h) and Br-82 ($t_{1/2}$ 35.9 h). Other long lived nuclides contributed only a few percent to the total counting rate. Fission product gases were undetectable.

6.4 Fuel Examination

6.4.1 Fouling Film

When the fuel stringer first arrived at the Universal Cells, the fuel bundles were separated and the filler pieces were removed to permit observation of the channels between the three elements. No obstruction was observed. The bundles and filler pieces were then washed in CCl_4 to remove the thin film of HB-40 and the assemblies were examined visually. Each bundle was finally separated into individual components for subsequent measurements.

6.4.1.1 Appearance of Film

Figure 9 shows a view of the partially disassembled stringer while Figure 10 shows bundle DEE with the filler piece removed. The following observations were made:

(1) A thin, apparently uniform, film covered the surface of all elements in areas which covered the fuel.

(2) The end caps of the elements, i.e. the unfuelled portions, showed no, or much less film. For instance the end caps of all elements at the inlet end of the fuel string (the bottom end of bundle DEE) showed no film and a fairly sharp demarcation where the film began. As far as could be determined this line of demarcation coincided with the beginning of the fuel. The top end caps of the elements of bundle DEE showed a slight amount of film but much less than covered the bodies of the element (see Figure 11). The end caps of the elements of bundle DEA showed no distinctive line of demarcation where the film began or ended.

(3) The surfaces of the dummy bundle and of the filler pieces were covered by extremely thin film which was little more than surface discoloration. Machining marks etc. were clearly visible. No attempt was made to measure film thicknesses on the dummy bundle or on the filler pieces.

(4) Circumferential ridging could be seen on the sheaths, especially on the

elements of bundle DEE. These ridges, which are apparent in Figure 9, apparently mark interfaces between fuel pellets. Subsequent investigations showed that these ridges were not prominent enough for any measurement of ridge height to be made with apparatus available at that time.

(5) On the elements, the film appeared thinner on the fins than on the rest of the element. There was a tendency for the film to be cracked at the edge or base of a fin (See Figure 12). Also when the elements were separated, discontinuities could be seen where the fin of one element had been in contact with the body of another (See Figure 13).

(6) Figure 14 shows, under higher magnification, the typical rippled appearance of the surface of the film. This appearance is reminiscent of the appearance of the sandy bottom of a fast flowing stream. Again the height of these ripples could not be determined but microscopic examination of a cross section of the film (See Section 6.4.1.2 (c)) showed irregularities in the film thickness. If these irregularities correspond to the ripples, then the ripples were in the order of 20 μm high (Figure 15).

(7) During subsequent scraping operations it appeared that the film consisted of a lightly adhering top layer which could be scraped easily and a tightly adherent lower layer which was very difficult to remove. Microscopic examination of cross sections of film did not show two layers present normally and probably there was a gradual transition from one to the other rather than a sharp demarcation.

6.4.1.2 Film Thickness

Several methods of measuring film thickness were attempted. Results are recorded in Table 8.

(a) In the Universal cell, the diameter of an element was measured. Then the film was scraped from a small area on one side and the diameter was again measured. Finally an area 180° from the first one was scraped and the diameter remeasured. Since the film was very adherent and was hard to scrape off, some gouging of the metal of the sheath occurred and hence the precision of this method was only about ± 0.05 mm.

(b) During the scraping several flakes of film could be removed. The thickness of these flakes were measured under a binocular microscope at 120 magnifications. The precision of this method is about ± 0.005 mm.

(c) At a later stage in the investigation transverse samples cut from each

element were coated with Hysol resin, mounted, polished and examined microscopically in the metallurgy Dry Box Line. A typical cross-section of the fouling film is shown in Figure 15. In all specimens examined, the film showed light grey particles embedded in a grey brown matrix. The film thickness appeared to vary randomly, being mainly around the value quoted in Table 8 but varying between the limits shown. Figure 15 is typical of the variation in film thickness, which is probably associated with the rippled appearance of the film (see Section 6.4.1.1 (5)).

It is not possible to extract quantitative information from Table 8 but the following generalizations may be made.

(i) The film on the lower third of the element of the bottom (inlet) bundle was thinner than on the remainder of the elements. The film averaged 40 μm in thickness here but was about 70-80 μm over the remainder of the fuel string.

(ii) Careful examination of all elements cross-sectioned and submitted for metallographic examination indicated that although there was considerable non-uniformity of film thickness, there was no preferential build up on any of the elements. This is illustrated by Figure 16 which shows thicknesses as measured around the circumference of an element from the lower bundle and one from the upper bundle. Typical examples of unevenness and discontinuities of the film are shown.

6.4.1.3 Chemical Composition of Film

Samples of film which had been scraped from the surfaces of the elements were submitted for the following chemical analyses.

(a) X-ray Diffraction - The results, outlined in Table 9, indicate that Fe_3O_4 or γ-Fe_2O_3 were the main constituents of the film. Only traces of α Fe or FeC could be observed.

(b) Samples of the film were ignited by standard ashing techniques. In Table 9 the percentage ash is given which is defined as (100) (wt ash after ignition)/(wt original sample).

(c) The residue from the above ashing was analyzed spectroscopically. Fe was by far the major constituent of the ash. Table 9 shows the significant cations found: the remainder total less than 1 wt%.

(d) The carbon and hydrogen content of the film was determined on some films by the standard Pregl technique. Results are listed in Table 9.

(e) γ-ray spectra were taken on several samples of film. In all instances the major long lived activities present were Fe 59, Co 60 and Co 58 with lesser amounts of Cr 51 and Mn 54. No quantitative data were taken.

6.4.2 Dimensional Changes

Length and diametral measurements made on the bundles and elements are listed in Table 10.

The irradiation had produced no detectable change in the diameters of the elements. Actually, due to the scraping to remove film, a dimunition rather than an increase in diameter was recorded. Lengths of the bundles or elements had not changed by more than 0.4 mm in an overall length of over 600 mm.

6.4.3 SAP Examination

No detailed examination of the SAP sheaths was made. A longitudinal cross section of the bottom end cap of element DEC was made. The sample was prepared for metallographic examination by abrading on silicon carbide papers, followed by fine polishing on diamond impregnated cloths and subsequent etching in a solution of 0.5% HF.

Small discontinuities ($<$ 0.02 mm long) were observed along the pressure bond but otherwise Figure 17 shows the bond to be in good condition.

6.4.4 Fission Gas Release

Prior to cutting the elements open they were punctured and the fission product gases were pumped from each element using the method described by Morgan (14). The composition and amounts of fission gas released are shown in Table 15.

6.4.5 UO_2 Examination

In the metallurgy examination cell each element was coated in epoxy resin to prevent fouling film flaking off when the element was sectioned. The sheaths were cut with a high-speed milling cutter that did not damage either the fouling film or fuel. A description of the UO_2 and measurements of the area of discernible grain growth are included in Table 11. All grain growth areas and voids were displaced towards the outside of the bundle from the axis of the elements because of the flux distortion across the bundles. The extent of grain growth measured on pellet faces was larger than that measured in the interiors of pellets (see Section 8.1).

The cobalt-copper monitors were badly pitted especially on the surface nearest the SAP sheathing (Figure 18). However, the inside surface of the sheath at the monitor position showed no signs of reaction (Figure 19).

Typical cross sections discussed in Table 11 are shown in Figures 20, 21 and 22.

6.4.6 Burn-up Analyses

Samples taken from the fuel at the centre of each element were analysed for U-235, Pu-239 + Pu-240 and Cs-137 by methods described by Hart (15). From these analyses the total irradiation in megawatt-days per tonne of U was calculated by conventional methods assuming that 182 Mev/fission was absorbed as heat in the fuel. Table 12 shows the results obtained.

Because of the interaction between the Co monitors and the sheath any results obtained from them were unreliable and are not reported.

7. DISCUSSION OF FOULING

7.1 Increase in Pressure Drop Across Fuel

7.1.1 Initial Data

At the start of the irradiation the pressure drop across the fuel (ΔP) was measured to be approximately 2.8 kg/cm^2. The pre-irradiation prediction (1) was 5.5 kg/cm^2 but this figure included the ΔP in the test section itself which amounted to about 0.5 kg/cm^2. In addition this calculation was made from data in reference (16). Subsequent experiments (17) have shown that the turbulence loss factors included in that report are high and that the value of f_T is $\sim$1.0 rather than the quoted value of 2.3.

Using this value, and for the overall fuel string (2 bundles plus one dummy) using a value of the equivalent diameter De = 2 x 10^{-3}m, the ΔP may be calculated to be 4.27 kg/cm^2. Other data for this calculation came from Lane (16) and the Moody (18) plot was used. This is still high and to bring the calculation into line with the measured ΔP a value of De = 4 x 10^{-3}m would have to be used.

The shape of the fuel bundles and filler pieces is very irregular however and a better estimation would be to look at only the centre channel. The ΔP for this channel of course will be the same as the overall ΔP. The measured value of De (4 x area/wetted perimeter) for this channel is 4 x 10^{-3}m. If the following parameters are used a value of 3.5 kg/cm^2 may

be calculated.

Equivalent Diameter $De = 4 \times 10^{-3}$m

Reynolds Number $N_{Re} = 6.6 \times 10^{4}$

Flow velocity in channel $V = 10.2$ m sec^{-1} (Ref. 16)

Roughness $\epsilon = 2 \times 10^{-7}$m

Friction Factor $f = 0.019$

ΔP Turbulence $= 0.5$ kg/cm^2

ΔP Friction $= 3.0$ kg/cm^2

Total $\Delta P = 3.5$ kg/cm^2

7.1.2 Final ΔP

By the end of the irradiation the ΔP had risen to 4.2 kg/cm^2. The fuel was found covered with a film which was about 80 μm thick. Since the spacing between the elements was about 1 mm, this film would not have made a significant contribution to any pressure losses due to turbulence which are less than 15% of the total ΔP anyway.

Subtracting the turbulence losses and assuming that the dummy bundle did not contribute to the increase in overall ΔP, then the ΔP across the fuel only due to friction losses was about 3.2 kg/cm^2. For the unfouled string the friction losses for the two fuel bundles only were 1.85 kg/cm^2.

Now the ΔP (friction) is given by

$$\Delta P = \frac{f\, L V^2 \rho}{2\, g\, De}$$

where the letters have conventional meanings.

Thus if subscript 1 represents the unfouled state and 2 represents the fouled state

$$\frac{\Delta P_2}{\Delta P_1} = \frac{f_2}{f_1} \quad \frac{(V_2)^2}{(V_1)^2} \quad \frac{De_1}{De_2}$$

If attention is confined to the central channel only, a 80 μm film will increase V_1 by about 10% and decrease De by the same amount.

$$\text{then} \quad \frac{f_2}{f_1} = \frac{1}{1.3} \times \frac{\Delta P_2}{\Delta P_1} = \frac{1}{1.3} \times \frac{3.2}{1.85} = 1.33$$

Noting that N_{Re} will be unchanged and using $f_1 = 0.019$, then $f_2 = 0.025$. If De = 3.6×10^{-4} m, then from the Moody plot a value of the sheath roughness $\epsilon = 7 \times 10^{-6}$ m = 7 μm can be obtained.

This calculation was done on the assumption that initial and final temperatures and temperature distributions were the same. This is not strictly so because inlet temperatures were lowered to compensate for increased sheath temperatures. The above calculation contains many approximations and assumptions, but it was not felt that a more precise calculation was warranted.

Considering the approximate nature of this calculation the agreement of the calculated roughness with the observed value (Section 6.4.1.1) of 20 μm is reasonable. For instance in Figure 15, one photograph shows a variation of $\sim \pm$ 10 μm in the surface while the other shows an essentially smooth surface.

7.1.3 Δ P Increase During Irradiation

The Δ P data of Figure 7 are reproduced in Figure 23 along with sheath temperature data. These data indicate that there were two main periods during which the Δ P showed a significant rate of rise. These were from Aug. 26 - Sept. 3 and Sept. 23 - Oct. 7. These two periods occurred after the reactor had been started up after a prolonged shut-down. During both these periods both reactor and loop operation were rather erratic. During the remainder of the irradiation the ΔP stayed steady or showed only slow rates of rise.

In the previous sections it was shown that the increase in ΔP was due mainly to roughening of the surface, and although it is probable that the main deposition occurred during periods of rapid ΔP rise, evidence to support this must come from sheath temperature data rather than ΔP data.

7.2 Sheath Temperature Data

7.2.1 Normalization of Data

In Figure 7 both the inlet temperature and the sheath temperatures are varying and only qualitative information can be obtained. To obtain more quantitative data the following procedure was adopted:-

(a) Periods were chosen during which both reactor power and loop conditions such as flow, temperatures, etc., were steady for a period of at least 24 hours.

(b) During these periods, sheath temperatures were calculated, assuming that no fouling film was present. The surface heat flux in the vicinity of a given thermocouple was calculated from the calorimetric heat output from the fuel string and a knowledge of the thermocouple height and the thermal neutron flux cosine distribution in the NRX reactor. Surface heat fluxes were normalized to a given reactor power and heavy water height. From this surface heat flux and from the inlet temperature and an estimate of the bulk coolant temperature at the location of the thermocouple calculated as in Section 6.2.6, the temperature of the sheath surface was calculated using film heat transfer coefficients given in reference 16. Finally a small correction was made for the fact that the temperature in a fin will be slightly lower (~10° C) than the sheath temperature. The sheath temperatures calculated in this way assume that no fouling film was present but should all be normalized one to another and effects of heavy water height, fuel string power etc., removed.

(c) The difference between this calculated temperature and the temperature as actually read by the thermocouples was noted. Details of calculations are not shown here but values of $T_{meas} - T_{calc}$ for various sheath thermocouples are listed in Table 13 and plotted as a function of time in Figure 23.

7.2.2 Effect of Fouling Film on Sheath Temperature

The results indicate that early in the irradiation the measured sheath temperatures agreed reasonably well with those calculated for thermocouples No. 1 while the rest showed temperatures 10 - 40° C higher than calculated. Unfortunately, results were not obtained for the initial period of operation (Aug. 14-23) when no deposit would be present on the fuel. Thus by Aug. 29 a film may already have been present on the fuel. Thermocouple No. 1 does not indicate this but its readings were significantly lower than the others throughout the irradiation.

Whether or not a film had formed by Aug. 29, during the period Sept. 1 - 8 all thermocouple readings were relatively constant for t/c's Nos. 1, 2 and 6. Thermocouples 4, 10 and 11 showed sharp discontinuities in their output, but this is thought to be due to relative movement of the fuel elements (See Section 7.2.4) rather than to formation or removal of any fouling film. Thus the indication is that no significant fouling occurred during this period although some may have occurred before. This is borne out by the ΔP data.

From Sept. 8 to Sept. 30 reactor and loop operation were so

erratic that no meaningful results could be obtained. However by Sept. 30 the value $T_{meas} - T_{calc}$ had increased significantly for all thermocouples except No. 11, (which did not show a large increase until Oct. 21). By Oct. 6 this increase had become even more pronounced.

Figure 23 shows that this period of large increase in $T_{meas} - T_{calc}$ occurs during the same period that the significant ΔP increase occurred. Thus it can be inferred that the fouling film was being deposited at its highest rate during this period.

During the remainder of the irradiation, temperatures (except for thermocouple No. 11) did not change greatly and it can be assumed that fouling was occurring at a greatly reduced rate.

The most striking observation in that during periods of steady reactor and loop operation neither the ΔP nor the sheath temperatures showed much change. The two periods Oct. 7 - 20 and Nov. 6 - 20 illustrate this most clearly.

Thus it appears that fouling occurred during periods of erratic reactor or loop operation.

7.2.3 Fouling Film Heat Transfer Coefficient

From the start to the finish of the irradiation, Table 13 shows that the values of $T_{meas} - T_{calc}$ increased by a maximum of $\sim$55 - 60°C. That is, assuming constant inlet temperature, heat flux etc., the sheath temperatures at the end of the irradiation were about 60°C higher than they were at the start. Assuming a surface heat flux of 100 watts/cm^2 this would indicate that the heat transfer coefficient of the 80 μm thick film that was formed was about 1.7 watt/cm^2 - °C. Thus the thermal conductivity of the film in the region 350 - 400°C was very roughly 0.014 watt/cm - °C. This is a maximum value since no allowance has been made for any increase in heat transfer coefficient due to roughness.

7.2.4 Erratic Sheath Temperature

Figure 23 shows that for thermocouples 4, 10 and 11 there were often sharp changes in sheath temperature. These changes occurred quite suddenly for no apparent reason. It will be noted that these thermocouples are all located in "outer" channels between the fuel elements and the pressure tube.

It is believed that these sharp changes are a result of movement of the elements in the bundle relative to one another. Perhaps

bowing occurred but the experiment described in Section 6.2.6 indicated that bowing did not occur at that particular time. Any change in orientation of an element would have a more significant effect on the outer thermocouples than it would on the inner because channels are smaller and more easily blocked.

This behaviour has nothing to do with a fouling film since very similar behaviour has been observed during subsequent irradiations with similar fuel bundles where a fouling film did not occur (19).

7.3 PCFT Data

Figure 7 shows that at the start of the experiment PCFT numbers for the loop coolant were high, but by early September, operation of the clay column had reduced them generally to < 10 mg. However by this time the ΔP results indicate that the fouling film had started forming. During Sept. 1 - 13, while the PCFT was at or below 10 mg, both ΔP measurements and sheath temperatures indicated that no significant amount of fouling occurred.

The reason for the marked increase in PCFT from Sept. 14-18 is not clear. The clay column was operating and as far as is known there were no untoward events in the loop beyond the leakage of HB-40 from the metering pump in the clay column circuit (Section 5.6) which reached its maximum on Sept. 27. Subsequent tests have shown that HB-40 itself should not contribute to a high PCFT value (20) but impurities may well have been injected along with it.

Whatever the reason for the increased PCFT numbers, during the period when they were high (Sept. 14 - 24) the ΔP did not increase significantly. (Sheath temperature data are not available for this period). The ΔP increase started after the reactor shut-down of Sept. 18 - 22 and by this time the PCFT numbers were falling again to the 10 mg level. Thus there is no direct evidence to attribute the increased fouling rate to the increased PCFT of the coolant during this period.

From October 1 to the end of the irradiation the PCFT was generally below 10 mg and during this period the ΔP rose from 3.7 to 4.2 kg/cm^2. The values of $T_{meas} - T_{calc}$ for all thermocouples also all increased by 15 to 20°C.

Subsequent irradiations using smaller clay columns but with a flow rate 100 $kg/hr\text{-}dm^2$ rather than that of 0.25 $kg/hr\text{-}dm^2$ used in this test and operating at a temperature of at least 300°C, kept the PCFT of the loop coolant below 5 mg, and a fuel test using fuel very similar to that

used in this test and operating at the same ratings showed negligible fouling over a two month period (19). Hence the main conclusion that can be reached here is that PCFT values in the region of 10 mg, do not necessarily guarantee low fouling rates.

7.4 Composition of Fouling Film

The data in Table 8 show that the average thickness of the fouling film was 80 μm except on the lower end of the lower bundle where it was 40 μm.

Table 9 shows that the film was partially organic in nature and partially inorganic. The organic constituent is at present unknown. The only clue to its composition is the carbon hydrogen ratio which was reasonably constant over all parts of the film. The data of Table 9 show the atomic C/H ratio to be 2.0 ± 0.1. Actually this figure is probably a lower limit since there is a possibility that some of the hydrogen determined by the Pregl analysis may have been due to adsorbed H_2O.

The C/H ratio for terphenyl ($C_{18}H_{14}$) is 1.28 and for hexaphenyl is 1.38. Hence the organic phase was undoubtedly a highly polymerized and high molecular weight phase, but its insolubility made a molecular weight determination impractical.

Table 9 shows that carbon and hydrogen made up 35 ± 2 weight percent of the film.

The inorganic phase was mainly Fe_3O_4 or γ-Fe_2O_3. (Fe_3O_4 is more probable because of the reducing conditions present). The Al found present undoubtedly resulted from the scraping process which had to be used to remove the adherent layer. The source of the other minor impurities is not known but they may have been picked up as impurities during handling in the hot-cells.

From the Fe content of the ash and the ash content of the film, it can be calculated from the data of Table 9, that the Fe content of the film was 38 ± 4 weight percent. This would correspond to 53 ± 6 weight percent of Fe_3O_4 in the film.

Thus, if the presence of Al is assumed to come from scraping the sheath itself, the composition of the film was roughly 60 weight % Fe_3O_4 and 40 weight percent polymerized organic. Assuming a ratio of 4 between the densities of Fe_3O_4 and the organic phase, then the film would be, by volume, roughly 25% Fe_3O_4 and 75% organic.

Examination of the magnified cross sections of the film (Figure 15) shows that if the white particles are Fe_3O_4 and the greyish matte is organic material the appearance is not inconsistent with the above calculations. The size of the white particles is generally greater than 5 μm. This size is surprisingly large considering that the nominal pore size of the filters was 5 μm but it is quite possible that the particles visible represent a growth phenomenon in the film itself whereby smaller, perhaps colloidal particles or Fe_3O_4 or Fe complexed with organic molecules, are transferred to the film from the coolant and there grow to the larger sized particles observed.

7.5 Method of Formation of Fouling Film

This experiment provided no direct evidence of the means by which the film was deposited and hence any discussion must be rather speculative. There is some indirect evidence however which is not inconsistent with present theories (21).

The average film thickness was 80 μm and the area of sheath over the fuel was 2.08×10^3 cm^2. Hence the volume of the film was roughly 17 cm^3 and the volume of polymerized organic was 13 cm^3 (Considering that some 500 litres of coolant were circulating in the loop, a negligible fraction was polymerized to form the organic part of the film).

Assuming that the film was 25% by volume Fe_3O_4 then the weight of Fe present was ~22 grams. Table 5 shows that the coolant contained usually ~3 ppm Fe, or a total of 1.2 g Fe. There were higher concentrations for short periods but the pressure drop and sheath temperature data indicate that the film was formed over a period of time. Hence the conclusion may be reached that the figure of 3 ppm represented a steady state concentration of Fe in the coolant and that Fe arrived at the fuel surface by a mass transfer process, probably from piping walls. There is no evidence to indicate whether this transfer occurred by a transfer of particles, colloidal particles or by true solution or complexing of Fe atoms.

The other point of interest is that the film was not deposited continuously. Apparently while conditions were steady the film growth rate was negligible, but during periods of erratic operation either of the reactor or of the loop, deposition rates were significant. The reason for this is not clear but may be associated with easier removal of oxide from surfaces by thermal shock, etc.

8. UO_2 BEHAVIOUR

8.1 Grain Growth

The UO_2 structure, described in Table 11, is similar to that found in UO_2 irradiated in the pressurized water loops (22) if the higher surface temperature of the fuel in the organic loop is taken into consideration. The discrepancy between grain growth areas measured on pellet faces and those in pellet interiors was probably a reflection of the original grain size distribution in the as-sintered pellets. Metallography of unirradiated pellets showed that the diameter of grains varied from an average of 32 μm at the center to 15 μm near the edges. The extent of grain growth can be readily measured when the initial grain size is 20 μm or less, but for material of larger grain diameter the change in size is very difficult to detect. For this reason the grain growth measurements taken on pellet faces where the initial grain size was 15 μm or smaller are considered more reliable and have been used in subsequent calculations.

8.2 $\int \kappa d\theta$

The derivation and use of the parameter $\int_{T_1}^{T_2} \kappa(\theta)d\theta$ where $\kappa(\theta)$ is the thermal conductivity of the oxide at temperature θ, and T_1 and T_2 are the limits of integration have been described by Robertson et al (23, 24). Subscripts s, g, m and o are applied to T to express temperatures of the surface, of just discernable grain growth, of the oxide melting point and of the oxide axis respectively.

The heat ratings of individual elements given in Table 14 were calculated from the data of Table 12 and 14. Maximum and minimum values for $\int_{400°C}^{To} \kappa d\theta$ and $\int_{400°C}^{Tg} \kappa d\theta$ were calculated with respect to two estimates for the heat transfer coefficient across the fuel-sheath interfaces. These estimates of 0.4 and 1.1 w/cm^2°C, were made on the basis of experience from other tests (25) and should roughly correspond to contact at zero pressure and at sheath-deforming pressure respectively. The values of $\int_{400°C}^{Tg} \kappa d\theta$ for elements, DEC, DEF and DEH calculated with a fuel-sheath transfer coefficient of 1.1 w/cm^2°C are in much better agreement with previous AECL tests (26) where $\int_{400°C}^{Tg} \kappa d\theta$ was found to be 30 $\pm$ 3 w/cm than those calculated for 0.4 w/cm^2°C. We have calculated UO_2 volume average temperatures and UO_2 thermal expansions for both values of the fuel-sheath transfer coefficient. The average oxide temperature, assuming a heat transfer coefficient of 0.4 w/cm^2°C, was 1180°C while that, assuming a heat transfer coefficient of 1.1 w/cm^2°C, was 1010°C. The corresponding oxide diametral expansions, assuming no restraint, were 0.0073 cm and 0.0062 cm. If we consider the cold diametral clearance, 0.010 - 0.015 cm, and the SAP diametral expansion

at operating temperature, 0.0065 cm, we see that the fuel should not have stressed the sheath by simple expansion. This is consistent with the bulk of the observations in Table 10. A mechanism other than simple expansion is required to explain the sheath expansion at the centre of element DEB.

8.3 Fission Gas Release

The amounts of fission gas released from each element are compared in Table 15 with amounts predicted from a simple diffusion model (27). The diffusion values were calculated for two experimental values of D', the composite diffusion coefficient. For each element the percentage of xenon actually released is greater than that predicted from the diffusion model. This difference is probably owing to the changes in the UO_2 microstructure caused by the high fuel temperature (> 1500°C).

9. CONCLUSIONS

1. An experimental trefoil assembly of pressed and sintered UO_2 sheathed in SAP successfully underwent an irradiation of 2400 MWD/Tonne U (max) while cooled by organic coolant at an average temperature of roughly 310°C in the X-7 loop in NRX. Surface temperatures were as high as 460°C. Pertinent operating conditions may be found in Tables 1 and 14 and in Figure 7.

2. During the irradiation a film of approximately 80 μm thickness built up on the surfaces of the sheath which covered fuel. Negligible film was found on surfaces not covering fuel.

3. This film was roughly, by weight, 60% Fe_3O_4 and 40% polymerized organic coolant. Its net effect was to increase the pressure drop across the fuel by 50% and to increase surface temperatures of the sheath by about 60°C.

4. The increase in ΔP could be roughly correlated with an increase in surface roughness and the increase in sheath temperature corresponded very roughly to a fouling film heat transfer coefficient with a maximum value of 1.7 w/cm^2 - °C.

5. The fouling film did not form continuously. Differential pressure and temperature measurements indicated that during periods of steady operating conditions the deposition rate was very small and only seemed to increase during periods of erratic reactor or loop operation. There was no clear correlation between the film deposition and such variables as the ash content

and the PCFT number of the loop coolant. Ash contents were generally less than 3 ppm and except for the initial period and one other period during operation the PCFT was generally below 10 mg.

6. The SAP sheath showed no effects of irradiation.

7. Except for small apparent diameter increases at two out of eighteen planes measured the fuel elements and bundles showed negligible dimensional changes. The significance of these two measurements is not known.

8. The appearance of the uranium oxide from this experiment was similar to that of uranium oxide irradiated in pressurized water loops at almost the same heat ratings.

9. When calculated for a fuel to sheath heat transfer coefficient of 1.1 w/cm^2 - °C, values of $\int_{400°C}^{T_g} \kappa d\theta$ were in good agreement with values obtained from previous tests.

10. Fission gas release from the elements varied from 5.6% Xe released for a heat rating of 36 w/cm to 1.9% Xe released for 33.5 w/cm.

10. EPILOGUE

Subsequent tests to this have been carried out with similar fuel bundles at similar ratings and temperatures. The main difference has been that small clay columns operating at a temperature (300°C) and with a high through-put (100 kg/dm^2-hr) have been used in place of the large column with a slow through-put used in this test. The PCFT number was kept at 5 mg or less and the ash content of the coolant was normally 1 ppm or less. Irradiations over three month periods have shown negligibly small fouling films which did not affect either the pressure drop across the fuel or the sheath temperature.

ACKNOWLEDGEMENT

For a report of this type, with so many persons involved in various aspects of the irradiation it is virtually impossible to acknowledge individual efforts. The authors therefore express their indebtedness to the members of the following Branches of AECL outside of the Chemistry and Metallurgy Division for their continued cooperation throughout the experiment.

NRX Reactor
Reactor Loops
Chemical Operations
Reactor Technology

BIBLIOGRAPHY

1. Lane A. D. and Lew D. E. - Final Proposal for the Cooperative Long Term Irradiation of Trefoil Fuel Bundles in the X-7 Loop
AECL Report Exp-NRX-70901 (June 1961) (NFP).

2. Wilson C. and Hallam C. - Fabrication Data of SAP Sheathed Fuel Bundles Designed for Long Term Trefoil Irradiation in NRX Reactor
CGE Report R61 CAP45 (Exp-NRX-70903) (September 1961).

3. Ottevangers, J. H. - Thermocouple Instrumentation of Fuel for Long Term Trefoil Irradiation in NRX Reactor
CGE Report R61 CAP60 (Exp-NRX-70904) (November 1961).

4. Boxall D. and Standish J. W. - Mechanical Properties of Dispersion Strengthened Aluminium Alloys
CGE Report R61 CAP69 (January 1962).

5. Sawatzky A. - Progress Report January 1 - March 31, 1962, Chemistry and Metallurgy Division
PR-CM-29, p. 101 (1962) (OUO).

6. Thexton H. E. - "X-709 Latch Test"
AECL Report Exp-NRX-70912 (March 1963) (NFP)

7. Nishimura D. T. - Notes on Thermocouples for In Reactor Loop Systems and Irradiation Facilities
AECL Report RLI-7 (January 1962) (NFP).

8. Wilson A. H. and Delaney R. D. - Design Specifications for the NRX Organic Loop
AECL Report Exp-NRX-3905 (October 1959) (NFP)

9. Benson P. R. - Development of the Pyrolytic Fouling Tests for Organic Reactor Coolants
A. I. Report NAA-SR-7362 (November 1962).

10. Duerksen J. H. and Charlesworth D. H. - Use of Attapulgus Clay for Organic Coolant Purification
AECL Report CRCE-1131 (December 1962).

11. Charlesworth D. H. - AECL Report Exp-NRX-70603
To be published.

12. Bock I. E. and Boyd A. W. - Axial Flux Distribution in a Lattice Position in the NRX Reactor
AECL Report 1481 (March 1962)

13. Mackintosh W. D., Miller O. A. and Cornett L. J. - The Routine Determination of Biphenyl, ortho-, meta- and para- Terphenyl in OCDRE - Type Coolants by Gas Chromatography.
AECL Report CI-219 (April 1961) (NFP)

14. Morgan, W. W. , Jones R. W., Olmstead, W. J. The Determination of Fission Product Xenon Released by UO_2 in Fuel Elements.
AECL Report CRDC-969 (September 1960).

15. Hart R. G., Lounsbury M. and McKay C. D. - A Comparison of Methods of Determining Burn-up on Uranium Dioxide Fuel Test Specimens.
AECL Report CRDC-1001 (AECL-1176) (January 1961).

16. Lane A. D. - Data for X-7 Loop Fuel Calculations.
AECL Report FD-83 (September 1961) (NFP).

17. Thexton H. E. - Private communication.

18. Moody L. F. - Trans. A. S. M. E. 66 , 671 (1944).

19. Progress Report, July 1 - September 31, 1962 - Chemistry and Metallurgy Division
PR-CM-31 p. 155 (1962)

20. Bancroft A. - Private Communication.

21. Charlesworth D. H. - Fouling in Organic Cooled Systems
AECL Report CRCE 1096 (1963).

22. Robertson J. A. L., Bain A. S., Allison G. M. and Stevens W. H. - Irradiation Behaviour of UO_2 Fuel Elements, Nuclear Metallurgy Vol. VI p. 45 A. I. M. E. (November 1959).

23. Robertson J. A. L., Bain A. S. Booth A. H., Howieson J., Morison W. G. and Robertson R. F. S. - Behaviour of Uranium Oxide as a Reactor Fuel
A/Conf 15/P/193 (June 1958).

24. Robertson J. A. L. - $\int \kappa d\theta$ in Fuel Irradiations
AECL 807 (June 1961).

25. Ross A. M. and Stoute R. L. - Heat Transfer Coefficient Between UO_2 and Zircaloy-2.
AECL Report CRFD 1075 (June 1962).

26. Notley M. J. F. - Irradiation Performance of X-2-r,
AECL Report Exp-NRX-2404 (June 1961) (NFP).

27. Booth A. H. - A Method of Calculating Fission Gas Diffusion from UO_2 Fuel and its Application to the X-2-f Loop Test
AECL Report CRDC-721 (September 1957).

28. Progress Report, July 1- September 30th, 1960 - Chemistry and Metallurgy Division,
PR-CM-23 p. 118 (1960)

29. Progress Report, January 1 - March 31st, 1960 - Chemistry and Metallurgy Division
PR-CM-21 p. 160 (1960).

30. Progress Report - July 1 - September 30th, 1961 - Chemistry and Metallurgy Division,
PR-CM-27 p. 132 (1961).

31. Jones R. W. - Private communication

32. Wray, L. W. - The Determination of Fe in Terphenyl by X-ray Emission Spectroscopy, Applied Spectroscopy 16 no. 4 140 (1962).

TABLE 1

FUEL OPERATING DATA - MAXIMUM CONDITIONS AT 42 MW NRX POWER

PERIOD in 1961	TEMPERATURES °C			SURFACE HEAT FLUX	$\int \kappa d\theta$ w/cm	FUEL STRINGER POWER kw	BURN-UP MWD/T_eU
	COOLANT		SHEATH (a)				
	Fuel Inlet	Fuel Outlet					
15 Aug. - 13 Sept.	313	368	446	106	37.8	170	796
13 Sept. -18 Sept.	288	341	453	102	36.2	163	143
22 Sept. - 23 Oct.	304	350	452	93	33.2	149	824
27 Oct. - 20 Nov.	287	334	463	94	33.2	149	676
						TOTAL	2439
proposed conditions	304	359	450	113	44	181	

(a) Temperature as measured in fin. Sheath temperature is estimated to be ~10°C higher.

TABLE 2

BOWING TEST

REACTOR POWER (MW)	MODERATOR LEVEL (cm)	FUEL POWER (KW)	q'' at t/c 4 (w/cm^2)	MEASURED TEMPERATURES °C		T_c at t/c 4 (°C)	ΔT_f (T_{sh}-T_c) (°C)
				Coolant Inlet	Sheath at * t/c 4 (T_{sh})		
10.0	283	35.9	20.2	286	321	294	27
19.9	268	75.1	41.3	278	353	294	59
30.0	282	110.5	62.2	269	381	292	89
37.3	271	141.4	78.1	259	403	290	113
41.1	263	163.6	88.8	258	428	294	134
42.0	285	168.9	95.0	260	436	296	140

* Uncorrected for fin effect

TABLE 3

X-7 COOLANT COMPOSITION
(weight percent)

DATE	BIPHENYL	TERPHENYL			100 - $\sum$(a)	O/M RATIO	HB
		Ortho	Meta	Para			
16 Aug. 61	5.1	38.4	22.1	2.0	32.5	1.74	29.4
22 Aug. 61	5.0	37.0	21.3	2.0	34.7	1.74	
28 Aug. 61	5.6	37.2	21.3	2.0	33.9	1.75	30.4
5 Sept. 61	5.0	36.8	21.6	2.2	34.4	1.70	30.3
11 Sept. 61	4.7	35.1	20.6	2.1	37.5	1.70	28.0
18 Sept. 61	5.8	37.6	22.6	2.3	31.8	1.66	28.9
25 Sept. 61	4.6	34.0	19.9	2.0	39.5	1.70	31.4
2 Oct. 61	4.8	33.9	19.9	2.0	39.5	1.70	28.1
10 Oct. 61							30.1
14 Oct. 61	5.1	33.6	20.2	2.0	39.1	1.66	
16 Oct. 61	4.9	33.6	20.4	2.0	39.1	1.65	28.7
30 Oct. 61	5.1	34.6	21.1	2.0	37.2	1.64	31.1
6 Nov. 61	4.8	33.9	19.8	1.8	39.7	1.71	33.0
15 Nov.	4.5	33.1	19.3	1.7	41.4	1.72	31.8
21 Nov.	4.7	33.0	19.7	2.0	40.6	1.68	

(a) Represents difference between 100% and sum of biphenyl and three terphenyl weight percentages.

TABLE 4

DENSITY, VISCOSITY AND VAPOUR PRESSURE OF COOLANT

TEMPERATURE°C	DENSITY (g/ml)		VISCOSITY (c poise)		VAPOUR PRESSURE (kg/cm^2)
	5 Sept.	6 Nov.	5 Sept.	6 Nov.	5 Sept.
250	0.930	0.935	0.85	0.85	0.35
275	0.918	0.912	0.70	0.68	0.51
300	0.887	0.890	0.56	0.56	0.75
325	0.865	0.868	0.48	0.49	1.09
350	0.843	0.845	0.41	0.41	1.59
375	0.822	0.824	0.35	0.36	2.35
400	0.800	0.800	0.31	0.31	3.30

TABLE 5

IMPURITIES IN X-7 COOLANT

DATE	Fe ppm	PCFT mg
14 Aug. 61		7
15 Aug. 61	23	13
16 Aug. 61		28
17 Aug. 61		51
18 Aug. 61		28
21 Aug. 61		22
22 Aug. 61		33
23 Aug. 61		29
24 Aug. 61		8
25 Aug. 61		13
28 Aug. 61	3	17
29 Aug. 61		5
30 Aug. 61		8
31 Aug. 61	3	14
1 Sept. 61		0.1
5 Sept. 61	2.5	9
6 Sept. 61		0.3
7 Sept. 61	2.5	4
8 Sept. 61		10
11 Sept. 61	2	4
13 Sept. 61		10
14 Sept. 61	7	25
15 Sept. 61		15
18 Sept. 61	12	36
20 Sept. 61		16
21 Sept. 61	3	
22 Sept. 61		14
25 Sept. 61	3	19
27 Sept. 61		12
28 Sept. 61	< 3	
29 Sept. 61		7
2 Oct. 61	< 3	4
4 Oct. 61		7
5 Oct. 61	< 3	
6 Oct. 61		9
10 Oct. 61	4	
11 Oct. 61		9
12 Oct. 61	3	
13 Oct. 61		7
16 Oct. 61	< 3	4
19 Oct. 61	2	7
20 Oct. 61		4
30 Oct. 61	10	8
2 Nov. 61	3	5
3 Nov. 61		6
6 Nov. 61	3	11
8 Nov. 61		5
9 Nov. 61	< 2	
10 Nov. 61		7
15 Nov. 61	2	4
16 Nov. 61		3
21 Nov. 61	2	4

TABLE 6

DISSOLVED GAS CONCENTRATIONS

DATE	TEMPERATURES (°C)		GAS CONCENTRATIONS (cc (STP)/kg)					TOTAL
	Fuel Inlet	Surge Tank	H_2	N_2	CH_4	CO	"HC"(a)	
30 Aug. 61	240	170	12	307	1.1	0.2	13	334
6 Sept. 61	~310	182	33	445	18	2.0	50	548
10 Oct. 61	288	182	26	399	6.9	1.3	28	461
18 Oct. 61	288	182	27	383	9.7	1.4	79	500
17 Nov. 61	285	183	64	405	10	0.5	55	535

(a) Those gases condensed at liquid N_2 temperature but not at dry ice temperature at 10^{-3} mm Hg pressure

TABLE 7

RADIOACTIVITIES OF COOLANT

SAMPLE DATE	TIME	GROSS $\beta\ \gamma$ (counts/min-g)
15 Aug. 61	0513	4.97×10^4
24 Aug. 61	0848	2.26×10^3
25 Aug. 61	0850	1.16×10^4
28 Aug. 61	0918	1.90×10^4
31 Aug. 61	0855	1.30×10^4
5 Sept. 61	0926	1.57×10^4
7 Sept. 61	1315	1.01×10^4
11 Sept. 61	0903	8.83×10^3
13 Sept. 61	0915	2.07×10^4
25 Sept. 61	0856	1.57×10^4
29 Sept. 61	0845	1.09×10^4
2 Oct. 61	0900	9.52×10^3
6 Oct. 61	0900	8.61×10^3
10 Oct. 61	1325	9.63×10^3
12 Oct. 61	0900	1.09×10^4
16 Oct. 61	0918	2.18×10^3
19 Oct. 61	0920	8.47×10^3
2 Nov. 61	0900	5.89×10^3
6 Nov. 61	1014	4.17×10^3
9 Nov. 61	1322	6.68×10^3
15 Nov. 61	1345	7.61×10^3

TABLE 8

FOULING FILM THICKNESS

BUNDLE	ELEMENT	FILM THICKNESS (μm) SCRAPING PRECISION ± 50 μm	MEASUREMENT OF CHIPS PRECISION ± 5 μm		METALLOGRAPHIC SECTION PRECISION ± 1 μm	
			Range	Average	Range	Average
DEA	DEB	55				
Upper 1/3	DEC	85			40-100	75
	DED	75				
	DEB	35	± 5	50	40-120	80
DEA	DEC	75	± 5	85	50-120	75
Middle	DED	80	± 5	70	40-160	80
	DEB	65				
DEA	DEC	60			50-100	75
Lower 1/3	DED	75				
	DEF	40				
DEE	DEH	50				
Upper 1/3	DEJ	50			60-120	75
	DEF	25	± 5	50		
DEE	DEH	70	± 8	50	30-100	60
Middle	DEJ	40	± 18	45	50-120	65
	DEF	70			25-70	40
DEE	DEH	35				
Lower 1/3	DEJ	35			20-80	40

TABLE 9

ANALYSES OF FOULING FILM

FUEL ELEMENT	LOCATION	FILM COMPOSITION (wt %)			X-RAY DIFFRACTION DATA (a)			ASH COMPOSITION (wt % of ASH) (b)					
		Ash	H	C	Fe_3O_4 or γFe_2O_3	α-Fe	FeC	Fe	Al	Ca	Cu	Ni	Si
DEB	General Scraping	71.6			P	T	-	52.0	2.5	-	0.3	-	-
DEC	General Scraping	66.0			P	-	T	53.0	4.5	0.8	0.4	0.4	-
	Top (outer layer)	62.8			P	T	-	74.0	0.5	0.06	-	-	0.3
	Top	79.0			P	-	T	51.0	0.8	0.4	0.8	0.4	0.1
DED	General Scraping	73.4			P	T	-	53.0	2.0	-	0.3	-	-
	Top 1/3	70.5	1.3	32.8				50.0	-	0.02	0.02	0.04	0.02
	Middle 1/3	68.0	1.5	34.1				60.0	-	0.03	0.03	0.06	0.1
	Bottom 1/3	66.8	1.4	35.6				57.0	-	0.03	-	0.03	0.02
DEF	General Scraping	72.5			P	T	-	52.0	3.0	-	0.2	-	-
	Top 1/3	68.4	1.4	34.6				56.0	-	0.03	0.03	0.06	0.06
	Middle 1/3	69.2	1.4	32.5				59.0	-	0.03	0.02	0.05	0.07
DEH	Top (outer layer)	58.0			P	-	T	53.0	1.5	1.0	0.4	0.07	0.6
	General Scraping	67.0			P	-	T	52.0	2.5	0.6	0.3	-	0.2
	Top	68.5			P	T	-	58.0	1.5	-	0.09	-	-
DEJ	General Scraping	72.2			P	T	-	43.0	1.0	-	0.07	-	-

(a) P designates principal component
T designates trace component
- designates not detected

(b) - designates not detected

TABLE 10

DIMENSIONAL CHANGES IN ELEMENTS

	BUNDLE LENGTH (cm)			ELEMENT LENGTH (cm)			ELEMENT DIAMETER - TOP (cm)			ELEMENT DIAMETER - MIDDLE (cm)			ELEMENT DIAMETER- BOTTOM (cm)		
	Pre-Irrad.	Post Irrad. *	Change	Pre-Irrad.	Post Irrad. *	Change	Pre-Irrad.	Post-Irrad. *	Change	Pre-Irrad.	Post-Irrad. *	Change	Pre-Irrad.	Post-Irrad. *	Change
BUNDLE DEA	61.613	61.625-61.659	0.012-0.046												
Element DEB				60.960	60.988	0.028	1.5710-1.5728	1.5712	N.C.	1.5692-1.5715	1.5747	0.003-0.005	1.5679-1.5730	1.5699	N.C.
Element DEC				60.957	60.973	0.016	1.5631-1.5682	1.5638	N.C.	1.5662-1.5712	1.5666	N.C.	1.5677-1.5692	1.5691	N.C.
Element DED				60.960	60.968	0.008	1.5651-1.5677	1.5622	N.C.	1.5636-1.5662	1.5622	N.C.	1.5646-1.5667	1.5648	N.C.
BUNDLE DEE	61.631	61.646-61.666	0.015-0.035												
Element DEF				60.965	60.993	0.028	1.5692-1.5733	1.5675-1.5711	N.C.	1.5707-1.5738	1.5696-1.5716	N.C.	1.5733-1.5743	1.5762-1.5774	0.003
Element DEH				60.965	60.993	0.028	1.5677-1.5697	1.5679	N.C.	1.5667-1.5697	1.5660	N.C.	1.5667-1.5679	1.5648**	N.C.
Element DEJ				60.965	60.975	0.010	1.5634-1.5651	1.5648	N.C.	1.5636-1.5667	1.5666	N.C.	1.5646-1.5667	1.5640	N.C.

NOTE: In the diameter measurements the sheath surface was often gouged when scraping the film from the sheath, therefore most post-irradiation values are smaller than pre-irradiation.

* Corrected for temperature of sheath while in the Universal Cell.

** Difficult to get readings.

N.C. No change in dimension.

TABLE 11

DISPOSITION OF URANIUM OXIDE IN ELEMENTS

Bundle and Elements (1)	Grain Growth (2)	Av. Dia. of grain growth at mid-point (cm)	Central Void (2)	UO_2 Cracking
Bundle DEA	Equiaxed grain growth observed in the top pellets and in the bottom half of the elements. Short columnar grains surrounded the voids. Adjacent pellet faces had coalesced in the grain growth region of DEC. Dark concentric rings were found on pellet faces and in the interiors of pellets.	DEB 0.333 DEC 0.348 0.612 pellet face DED 0.272	Small central voids were found at the top and bottom of elements DEB and DEC. The bottom void in DEC was approximately 25 cm long. Element DED has a small void only at the bottom.	The UO_2 was cracked both radially and circumferentially.
Bundle DEE Elements DEF DEH DEJ	Equiaxed grain growth observed in the top half of the elements. Short columnar grains surrounded the voids. Dark concentric rings were found on pellet faces and in the interiors of pellets. Figure 20.	DEF 0.361 pellet face DEH 0.358 DEJ 0.485 pellet face	Small central voids were found at the tops of elements only. Figure 21.	Pellets with grain growth cracked radially and circumferentially; pellets without grain growth were randomly cracked. Figure 22.

(1) Centre line of reactor flux was between bundles DEA and DEE.

(2) Areas of grain growth and voids displaced from the element axis, see Section 6.4.5.

TABLE 12

CHEMICAL MEASUREMENT OF BURN-UP

Element	Pellet	Burn-up (MWd/tonne U)* From Cs-137	Burn-up (MWd/tonne U)* From Pu
DEB	14 & 15	2480	2430
DEC	16 & 15	2380	2300
DED	16 & 15	2430	2370
Average of Bundle DEA		2400	
DEF	14 & 15	2310	2160
DEH	13 & 15	2410	2250
DEJ	16 & 15	2240	2190
Average of Bundle DEE		2260	

* Based on 182 MeV/fission and reduced by 2% to compensate for end effects.

TABLE 13

SHEATH TEMPERATURE INCREASES

LOCATION	THERMOCOUPLE NO.	$T_{sheath(measured)} - T_{sheath(calc)}$ (°C)								$T_f - T_i$
		Aug. 29-31	Sept. 1-3	Sept. 6-8	Sept 30 -Oct. 1	Oct. 7-20	Oct. 29	Nov. 2-3	Nov. 6-20	
Inner channels Bundle DEA	1	1	1	3	39	52	56	58	62	~60
	2	20	21	23	57	66	75	74	76	56
	3	-	-	-	-	57	55	60	57	
	6		19	19	51	60	67	66	-	
Outer channels Bundle DEA	4	45	31	47	65	86	84	91	88	60 or 45
Outer channels	10	17	7	9	30	34	37	55	45	~40 or 30
Bundle DEE	11	31	7	32	33	39	55	60	66	57 or 30

TABLE 14

HEAT RATINGS OF FUEL ELEMENTS

Bundle	Element	Average Burnup at Center MWd/tonne U	Average Power Output KW	Linear Heat Output W/cm	Surface Heat Flux (Fuel to Sheath) W/cm^2	$\int_{T_s}^{T_o} \kappa d\theta$ W/cm	$\int_{400°C}^{T_o} \kappa d\theta$ W/cm		$\int_{400°C}^{T_g} \kappa d$ W/cm	
							(2)	(3)	(2)	(3)
	DEB	2462	28.0	485	109	35.2	43.7	37.7		
DEA	DEC	2345	26.5	459	103	33.3	41.3	35.8	34 (4)	30
(1)	DED	2408	27.3	473	106	34.4	42.4	36.9		
	DEF	2241	25.5	441	99	32.0	38.5	33.5	36 (4)	32
DEE	DEH	2336	26.6	460	103.5	33.4	40.9	34.9		
	DEJ	2223	25.1	435	98	31.6	38.1	33.1	34 (4)	30

(1) Center line of reactor flux located between bundles DEA and DEE.

(2) Calculated for a gap coefficient (Fuel to sheath) of 0.4 W/cm^2 °C.

(3) Calculated for a gap coefficient (Fuel to sheath) of. 1.1 W/cm^2 °C.

(4) Grain growth diameters measured for Pellet Faces at the mid-point of the elements.

TABLE 15

FISSION GAS RELEASE DATA

Bundle	Element	Gas Released (ml at STP)			Xe 136/ Xe 134	Fission Xe[1] Produced ml at STP	Percent Xe Released %	$\int_{400°C}^{T_o} \kappa d\theta$ [2] W/cm	Predicted Percent Xe Release from Diffusion % [3]
		He	Ar + Kr	Xe					
DEA	DEB	1.535	0.379	2.683	1.347	59.1	4.5	37.7	0.58 [4] - 1.1 [5]
	DEC	0.488	0.784	3.100	1.339	55.6	5.6	35.8	0.4 - 0.78
	DED	1.682	0.2628	1.397	1.338	57.4	2.4	36.9	0.5 - 0.94
DEE	DEF	1.244	0.1696	1.038	1.340	53.5	1.9	33.5	0.23 - 0.44
	DEH	0.818	0.203	1.335	1.342	55.8	2.4	34.9	0.32 - 0.64
	DEJ	0.9785	0.232	1.127	1.339	52.8	2.1	33.1	0.20 - 0.40

(1) Calculated using Average Burnup in Table 14.

(2) Values are from Table 14.

(3) Based on an activation energy for diffusion of Xe in UO_2 of 90 k cal/mole.

(4) Calculated for a D' of 0.824×10^{-11}.

(5) Calculated for a D' of 1.83×10^{-11}.

FIGURE 1

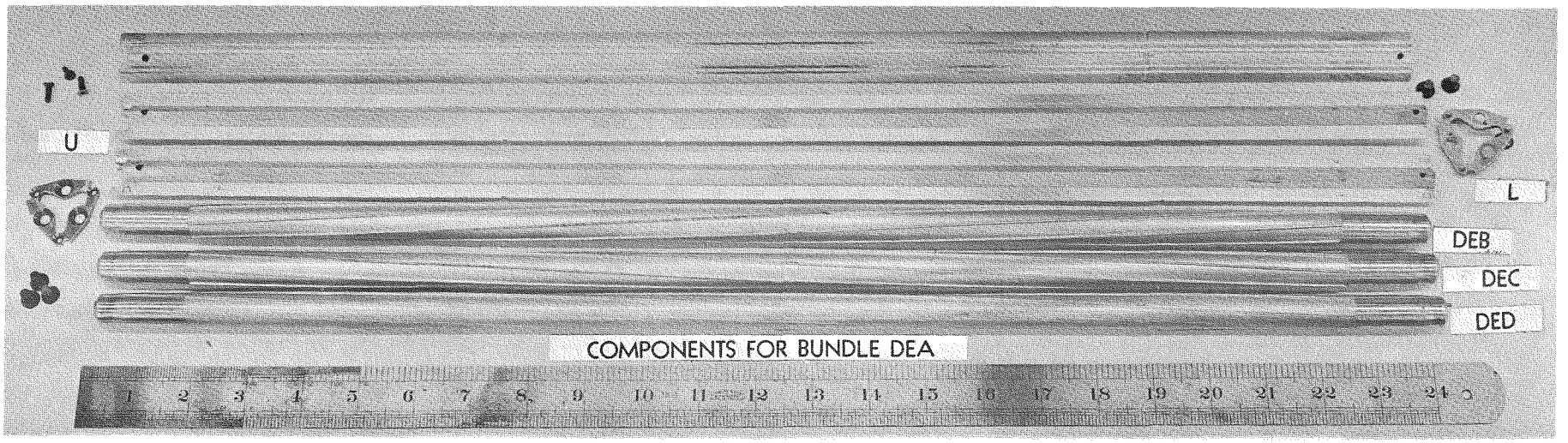

Bundle DEA disassembled, showing filler pieces at top and fuel elements below. End plates are at either side.

FIGURE 2

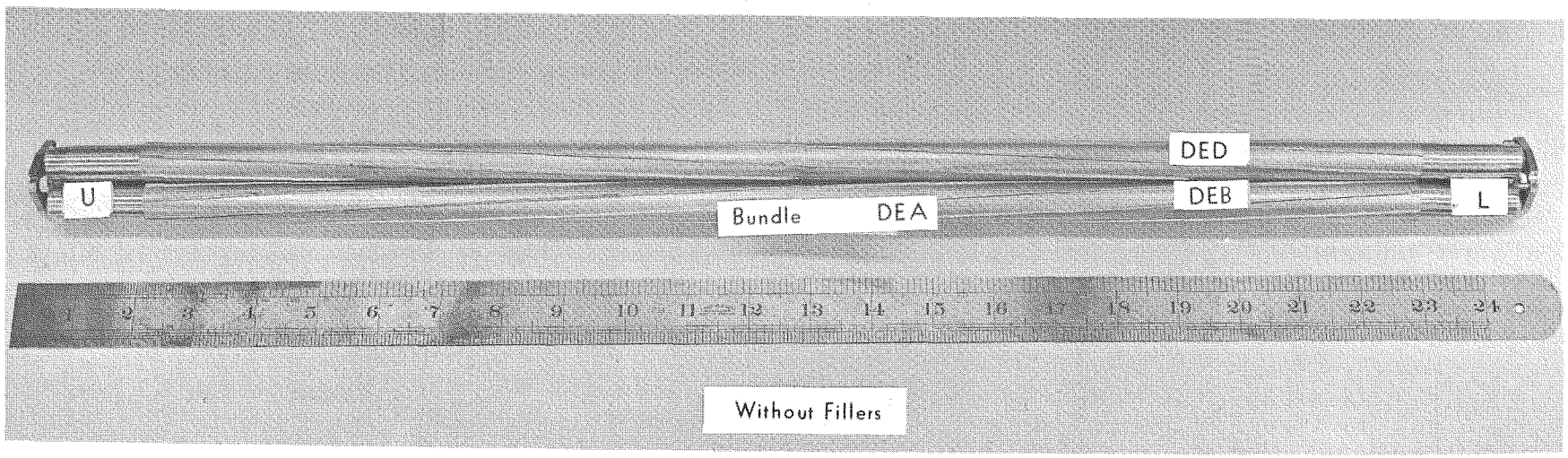

BUNDLE DEA WITHOUT FILLER PIECES

FIGURE 3

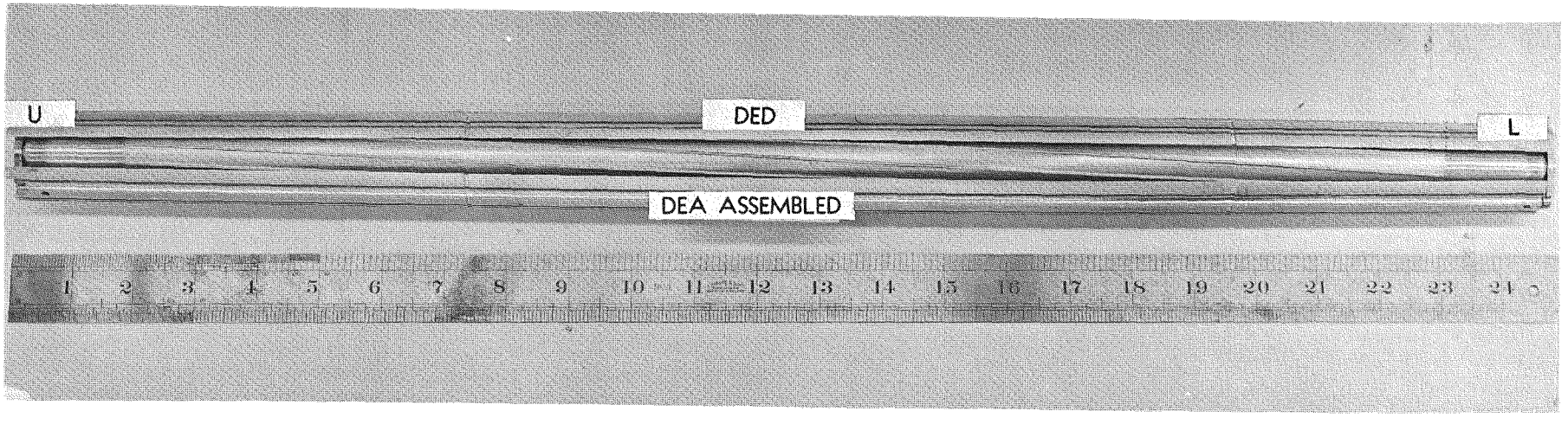

BUNDLE DEA ASSEMBLED

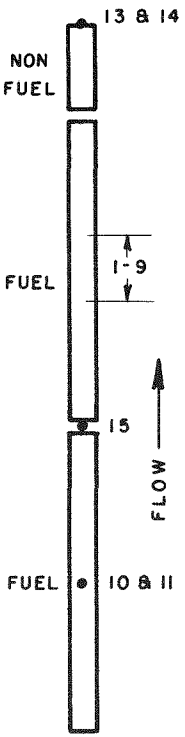

BUNDLE DEA

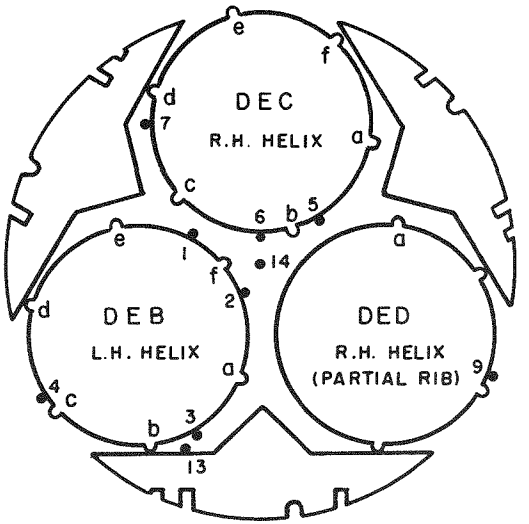

TOP FUEL BUNDLE IN STRING

BUNDLE DEE

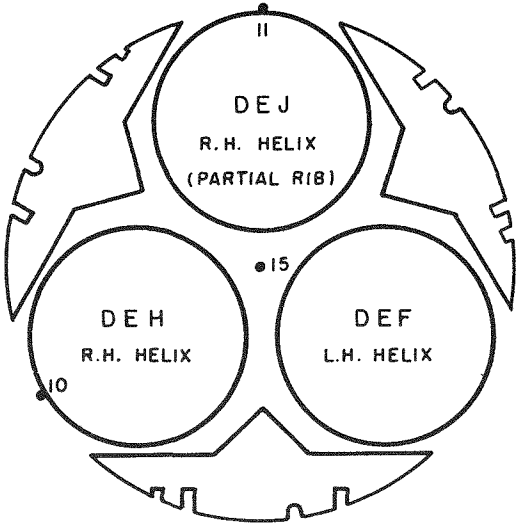

BOTTOM FUEL BUNDLE IN STRING

FIG. 4

• LOCATION OF MEASURING JUNCTION

T/C	FIN	DEPTH FROM END-CM	BUNDLE	ELEMENT
1	a	25-4	DEA	DEB
2	b	33	DEA	DEB
3	c	24	DEA	DEB
4	e	33	DEA	DEB
5	f	30	DEA	DEC
6	a	22	DEA	DEC
7	b	32	DEA	DEC
9	a	30.5	DEA	DED
10	a	30.5	DEE	DEH
11	a	30.5	DEE	DEJ

NOTE : GROOVES IN FILLER PIECES ARE FOR CARRIAGE WIRES AND THERMOCOUPLES.

THERMOCOUPLE LOCATION

EXP-NRX-70911

FIG. 5 EXP - NRX - 7091I

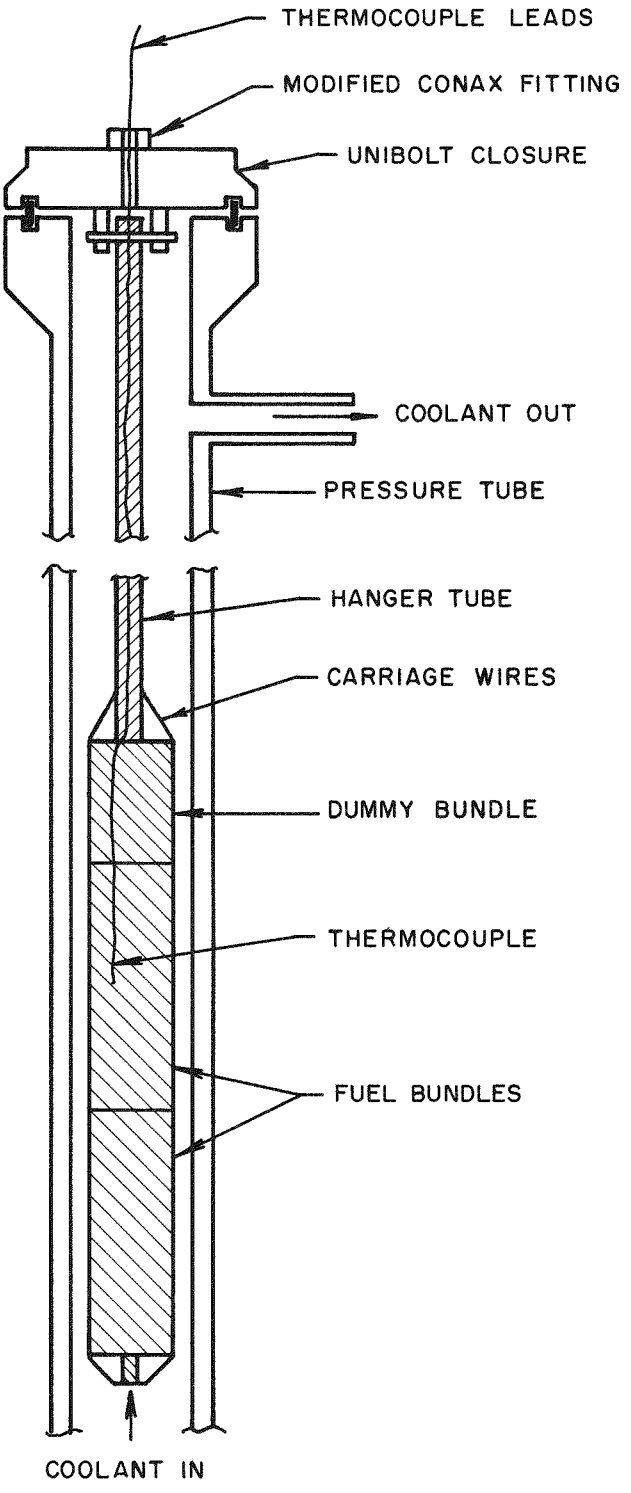

SCHEMATIC REPRESENTATION OF X - 7 LOOP TEST SECTION & X - 709 EXPERIMENTAL ASSEMBLY.

ADSORPTION COLUMN AND FILTER CIRCUIT

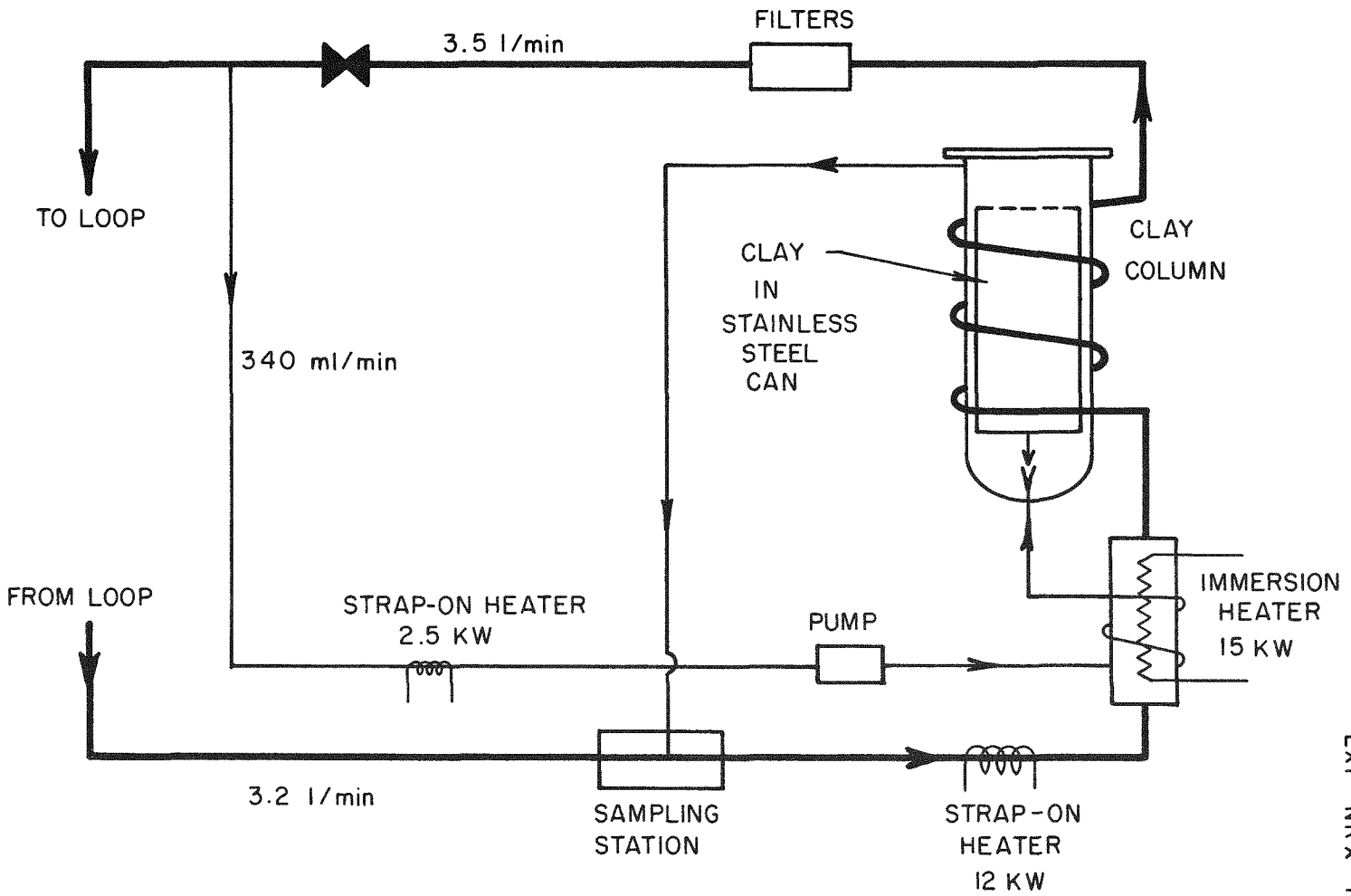

FIG. 6

EXP-NRX-70911

FIG. 7

OPERATING PARAMETERS

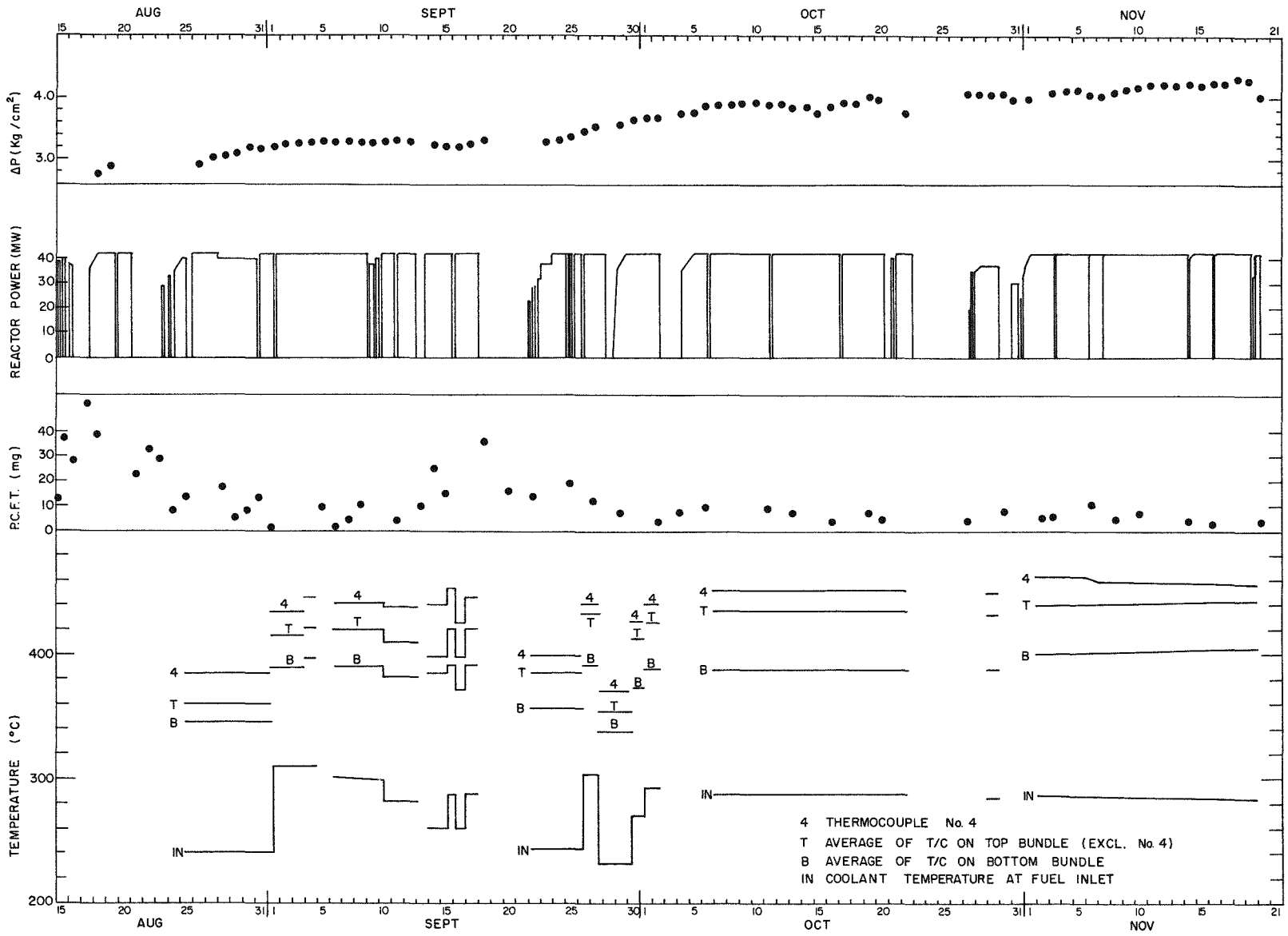

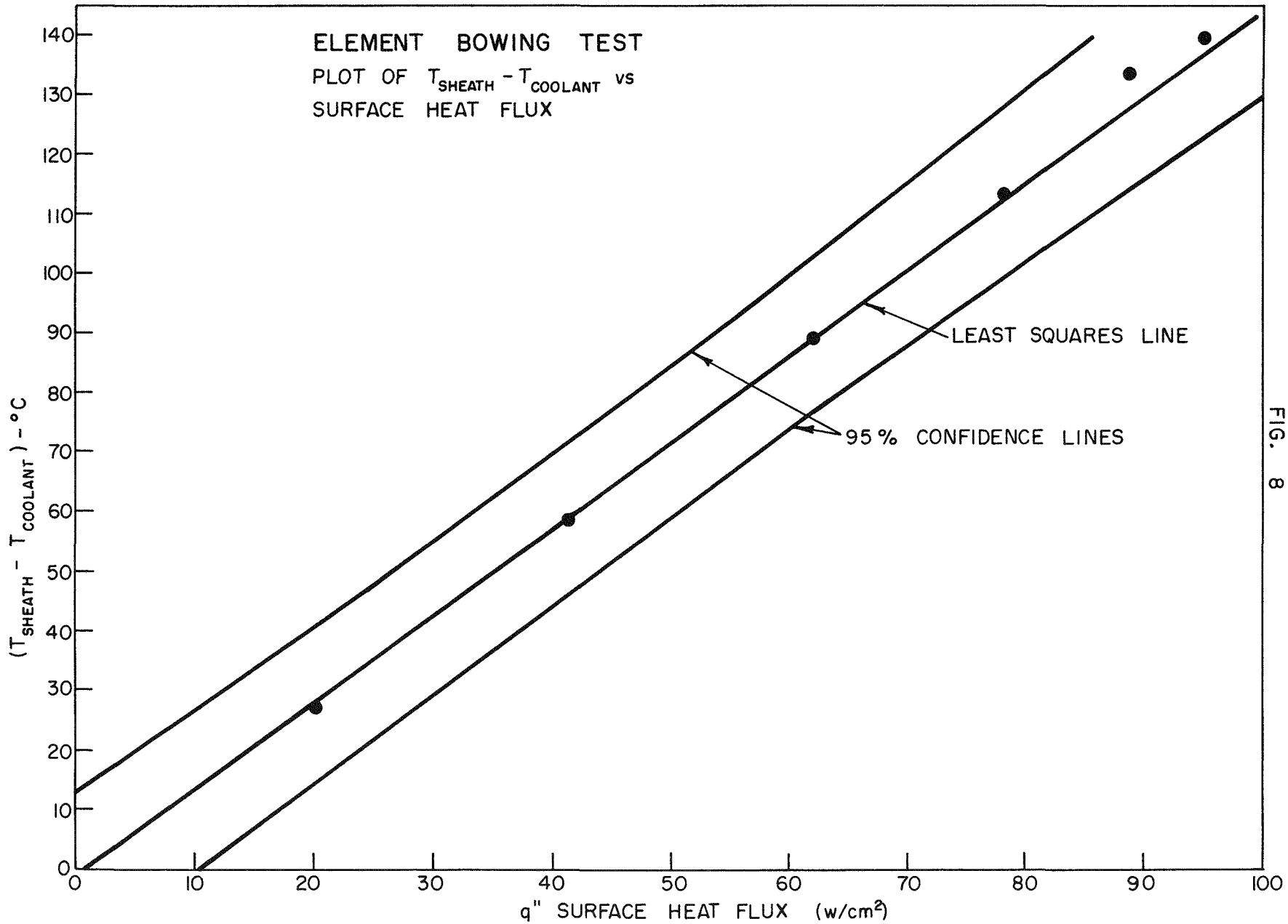
ELEMENT BOWING TEST
PLOT OF $T_{SHEATH} - T_{COOLANT}$ VS
SURFACE HEAT FLUX
LEAST SQUARES LINE
95 % CONFIDENCE LINES
$(T_{SHEATH} - T_{COOLANT})$ - °C
q" SURFACE HEAT FLUX (w/cm²)
0
10
20
30
40
50
60
70
80
90
100
110
120
130
140

FIG. 8

FIGURE 9

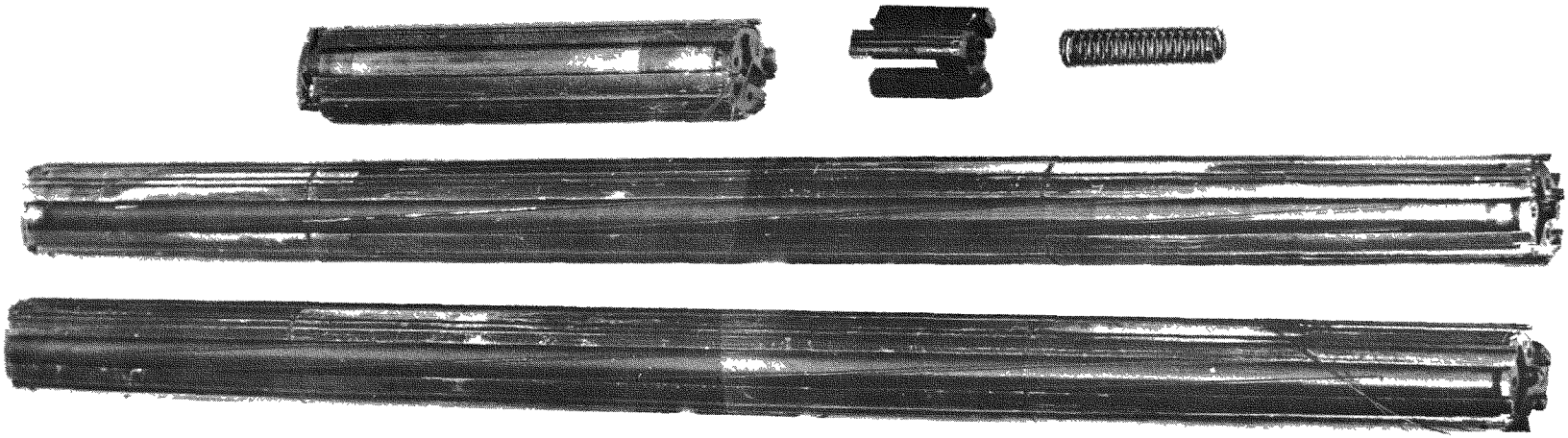

Composite photograph of partially disassembled fuel string after irradiation

Top Non-fueled bundle, Upper carriage spider and carriage spring

Centre Bundle DEA - Element DEC is visible

Bottom Bundle DEE - Element DEH is visible

Flow was from left to right over all components

Figure 10

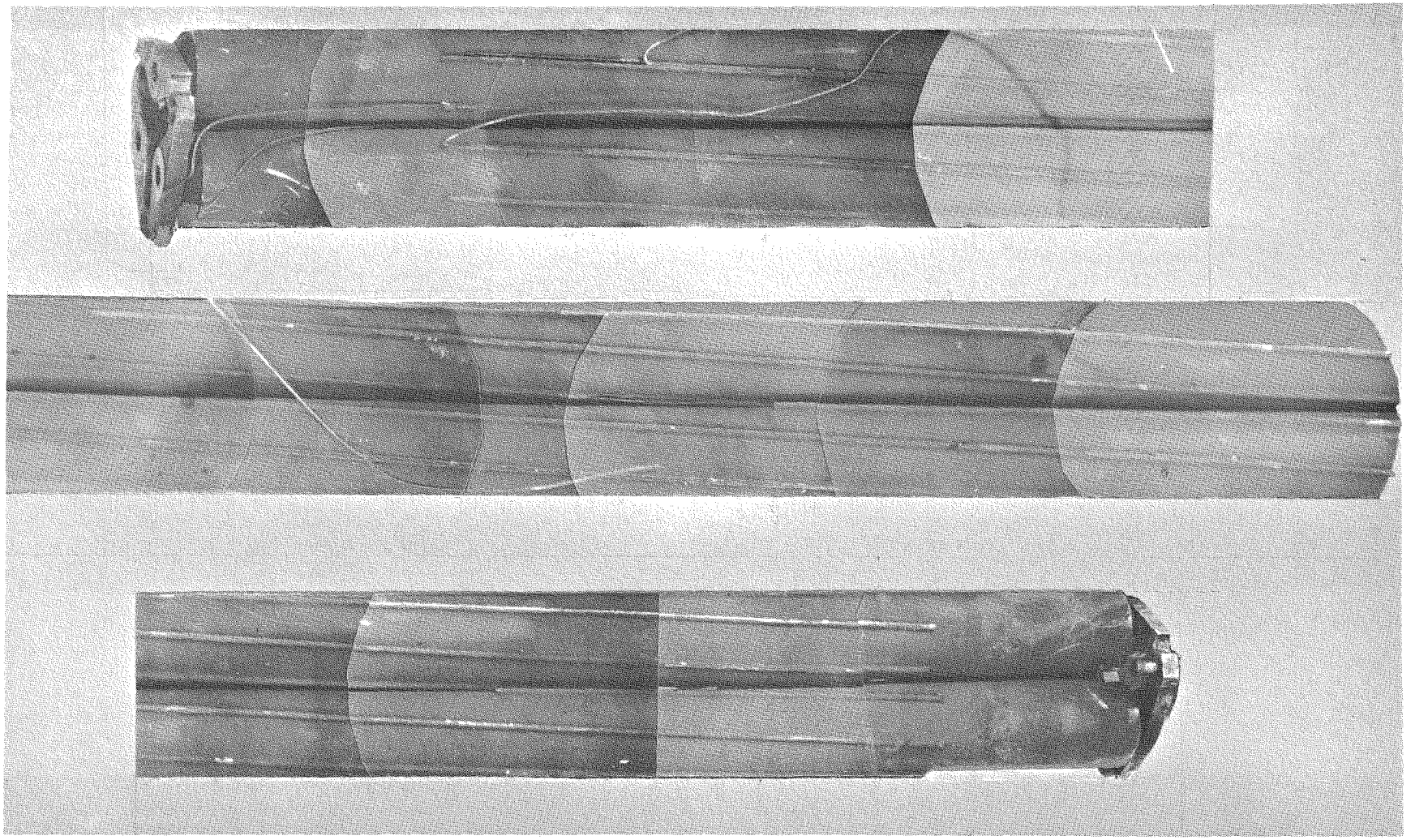

Composite photograph of bundle DEA with filler pieces removed
Flow from left to right

FIG. 11

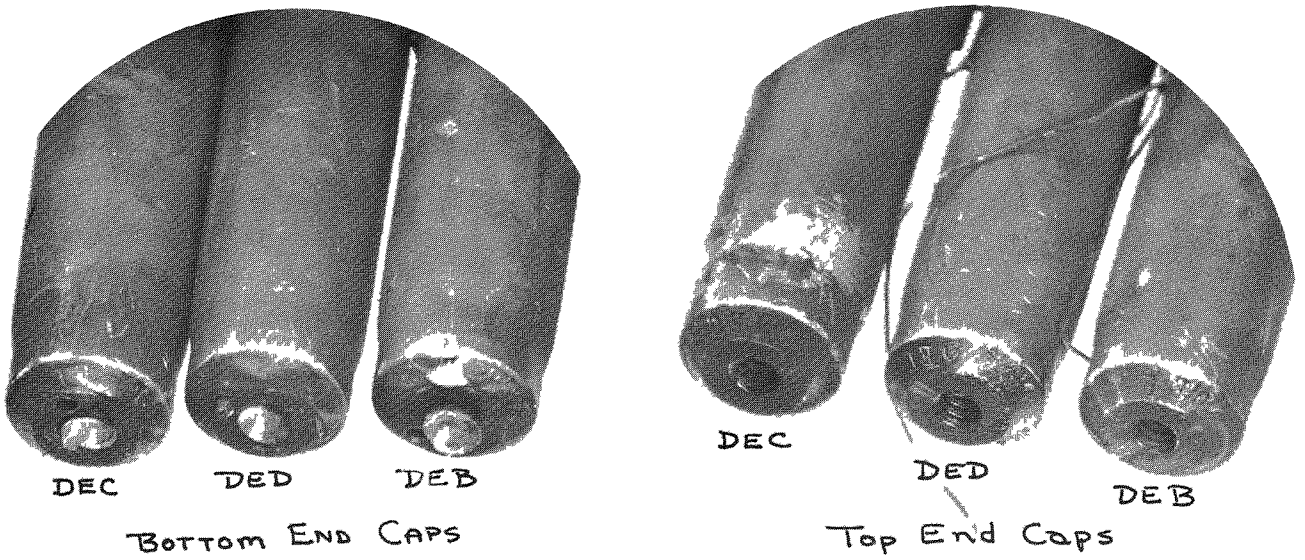

BUNDLE DEA

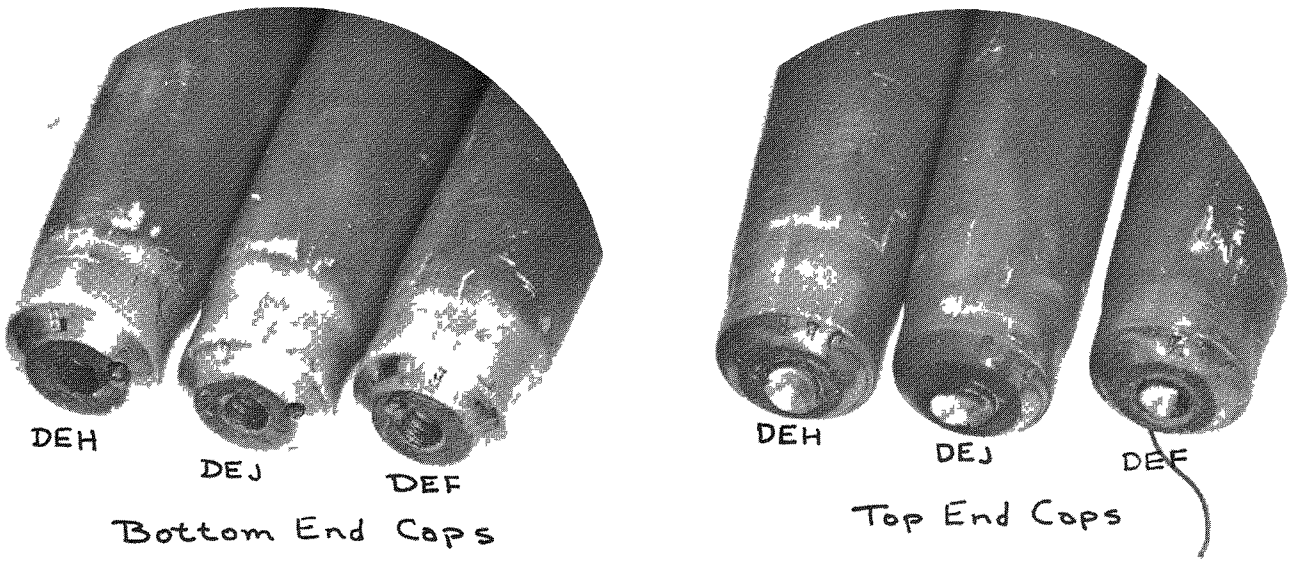

BUNDLE DEE

END CAP FOULING

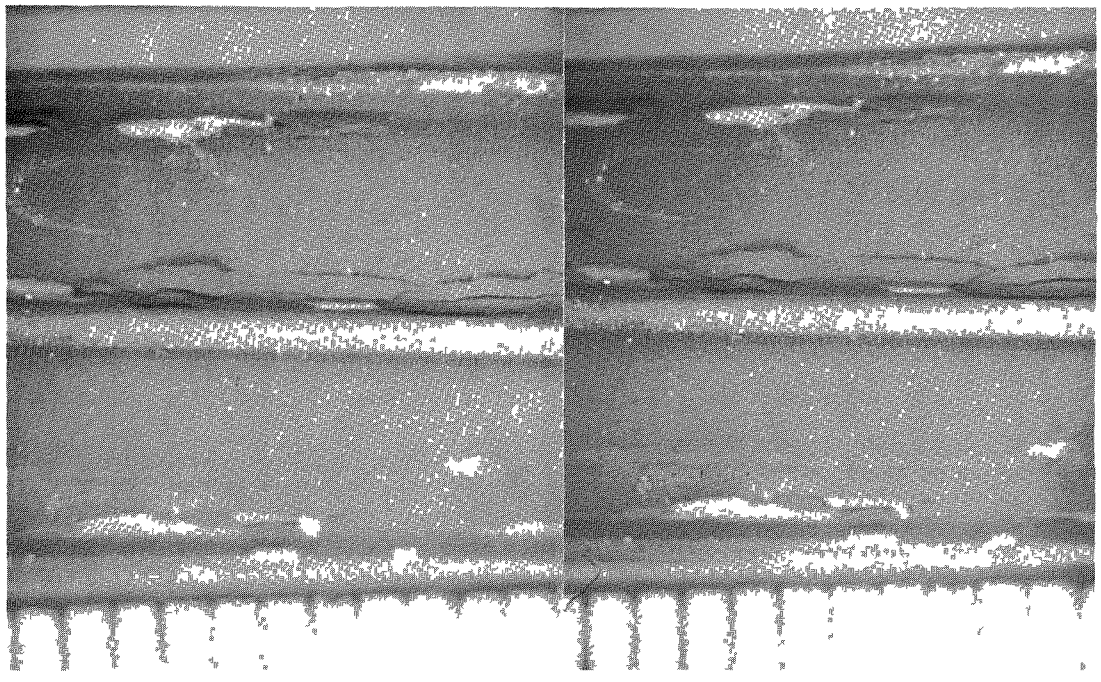

FIGURE 12 Cracked layer of fouling film next to fins on Element DEH. (stereopair)
Magnification 4X. Reference No. 6215

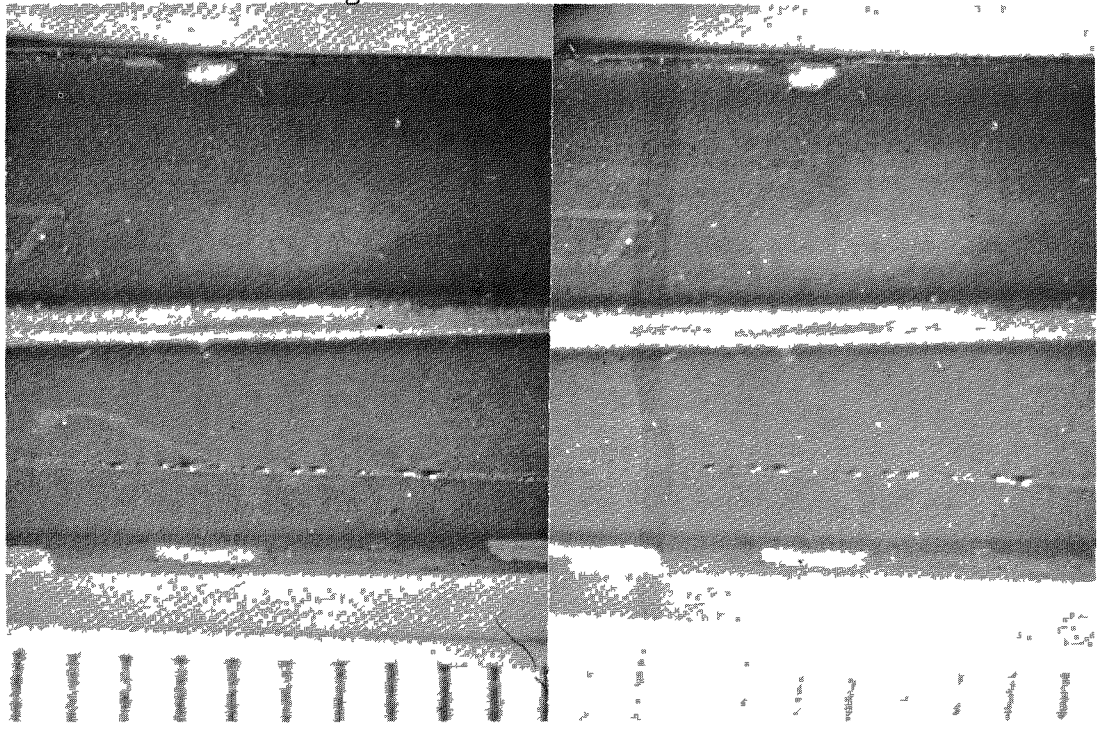

FIGURE 13 Stereopair showing line where fin of another element came in contact with the sheath of element DEH.
Magnification 4X. Reference No. 6216

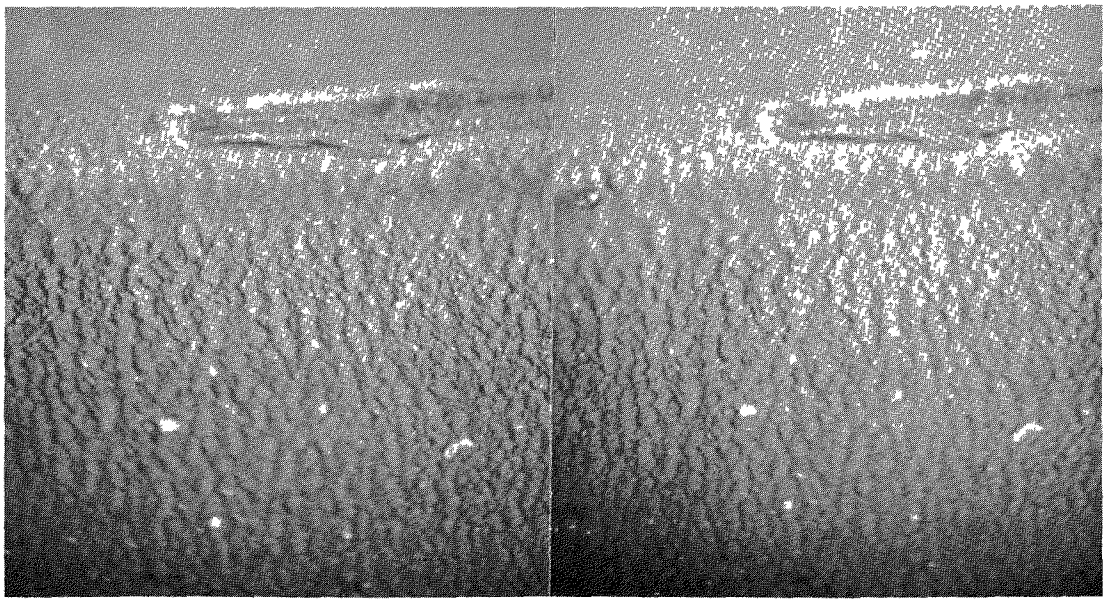

FIGURE 14 Wrinkled surface of the fouling film, Element DEB. Magnification 12X. Reference No. 6228

FIGURE 15

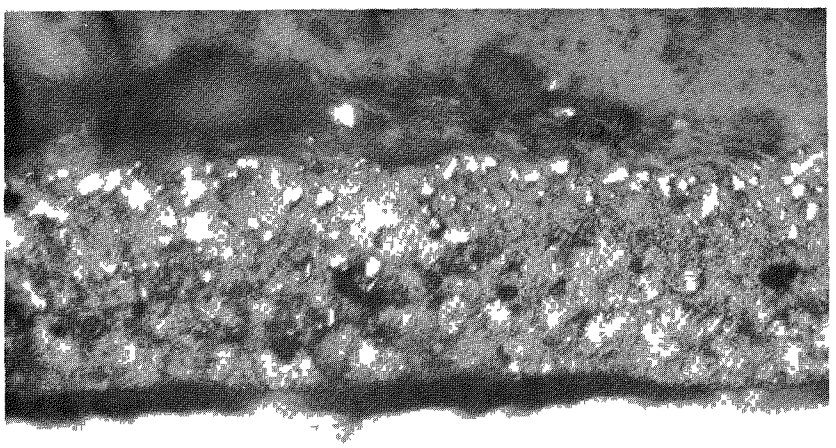

X500

Bundle DEE, Element DEJ

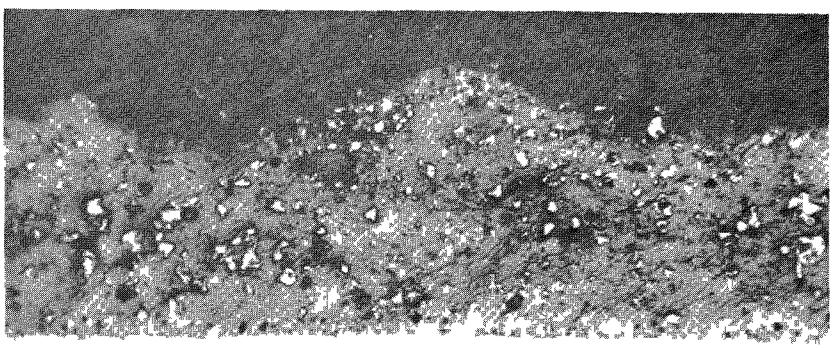

X500

Bundle DEA, Element DEC

Typical Cross Sections of Fouling Film

FIG. 16

ELEMENT DED - 29 cm FROM TOP

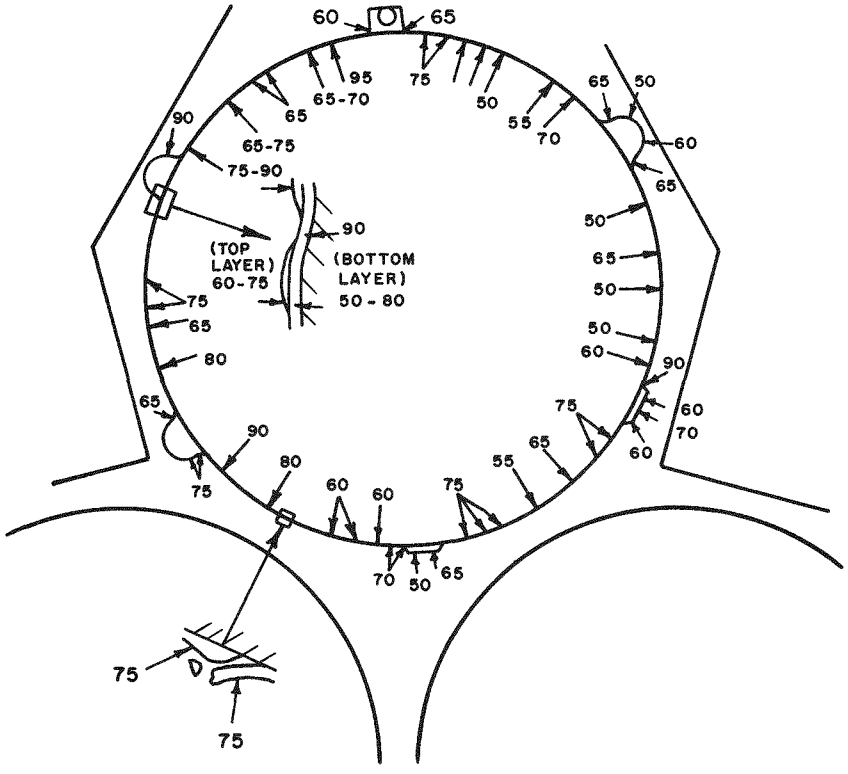

ELEMENT DEJ - 11 cm FROM BOTTOM

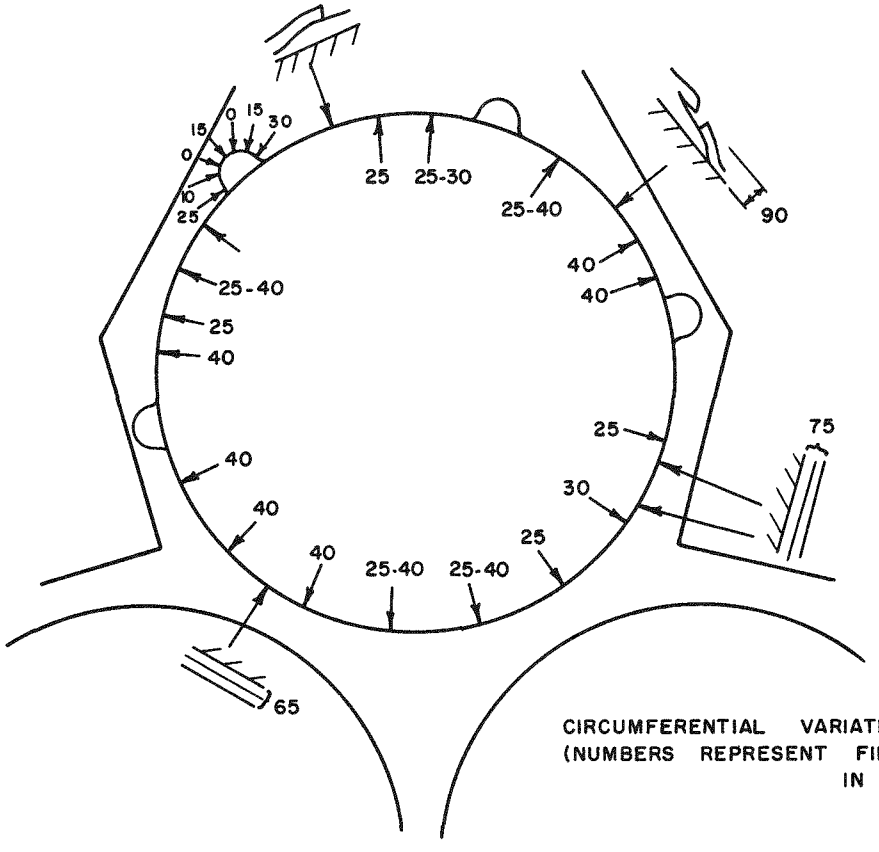

CIRCUMFERENTIAL VARIATION IN FOULING
(NUMBERS REPRESENT FILM THICKNESS IN MICRONS)

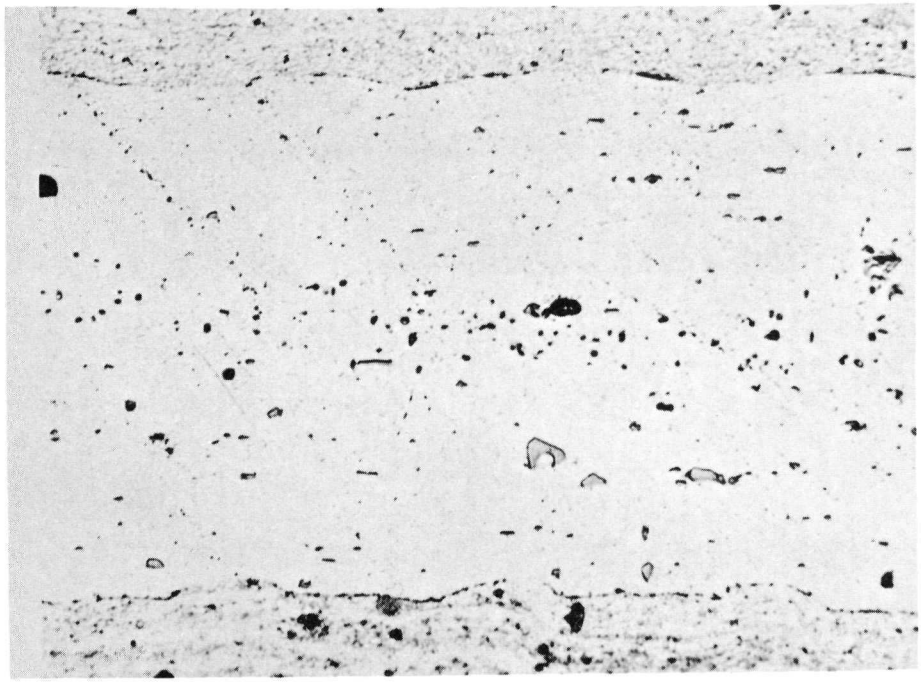

FIGURE 17

PHOTO MICROGRAPH SHOWING SMALL
AMOUNT OF POROSITY AND DISCONTINUITIES
AT SAP - 65 S interface

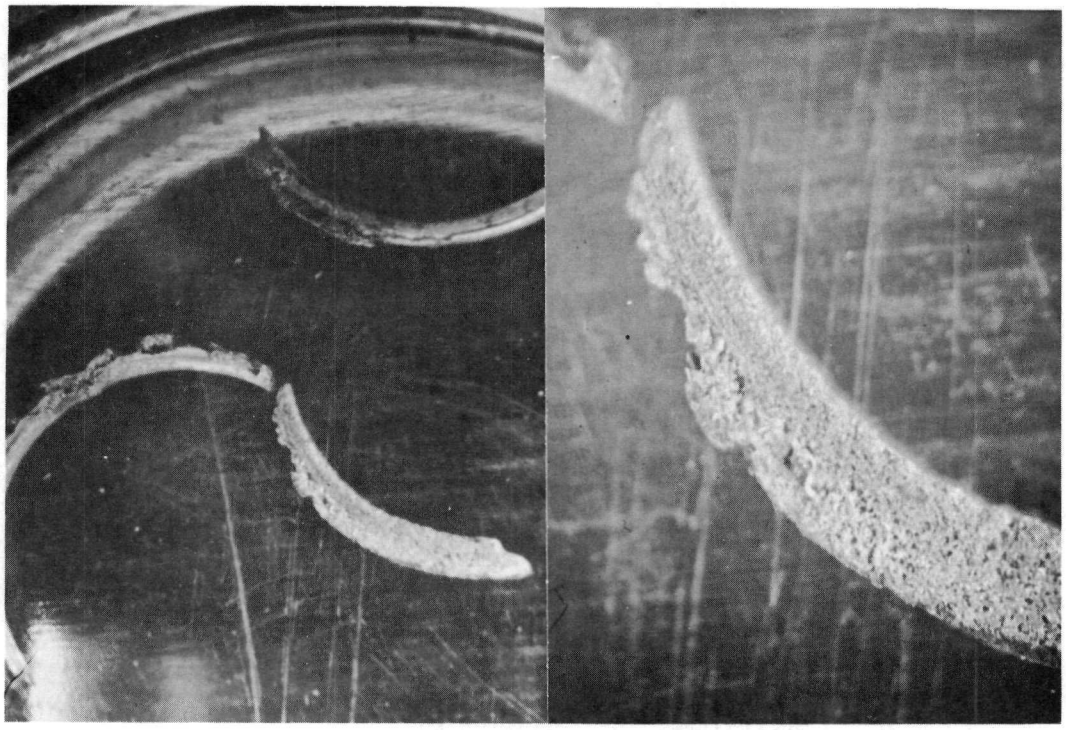

FIGURE 18 Cobalt-copper monitor from Element DEJ showing the extent of damage.
Magnifications 4X and 12X. Reference Nos. 6283, 6284.

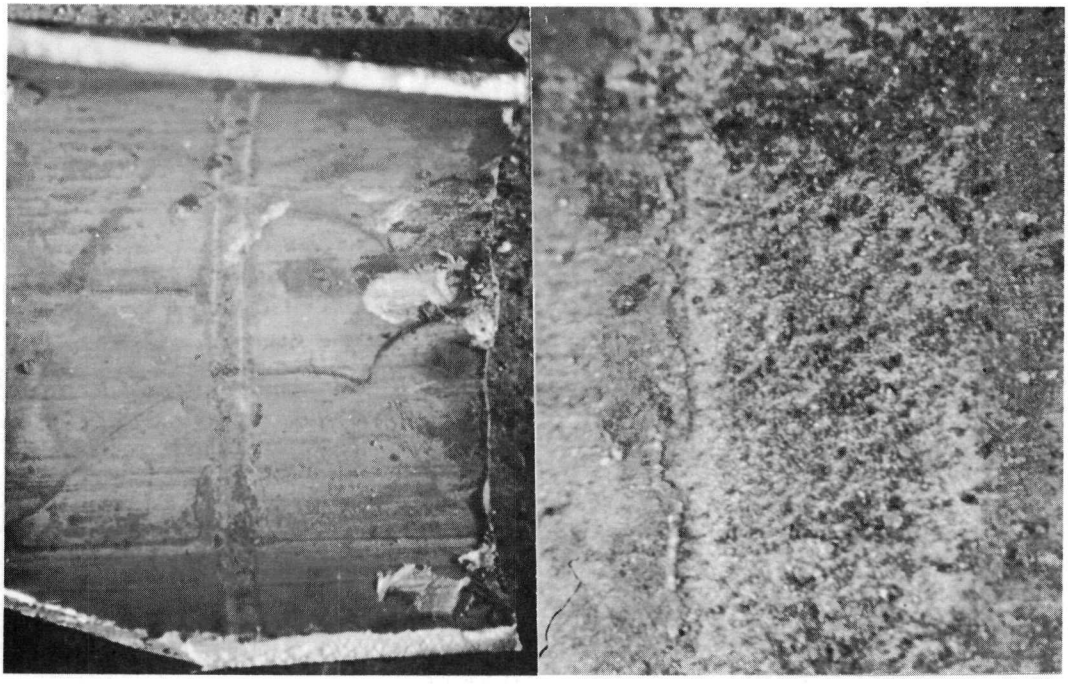

FIGURE 19 Inside surface of sheath, Element DEJ, showing the vertical line which is the location of the monitor in Figure 18.
Magnifications 4X and 12X. Reference Nos. 6280, 6281

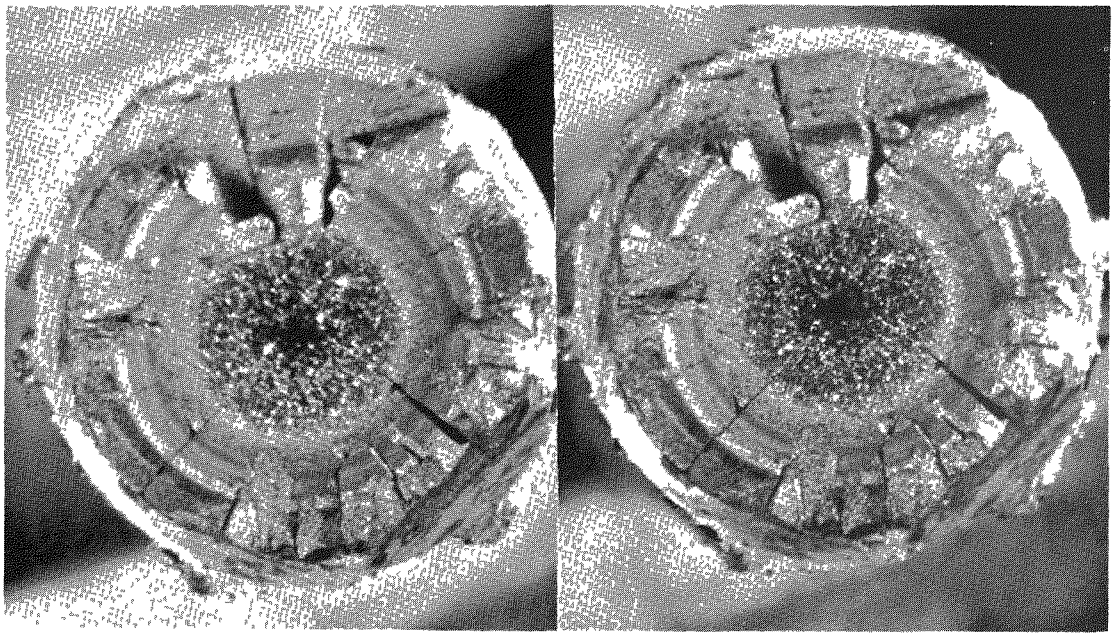

FIGURE 20 A pellet face, Element DEJ, showing equiaxed grain growth and dark concentric rings in the UO_2. (stereopair).
Magnification 4X. Reference No. 6271

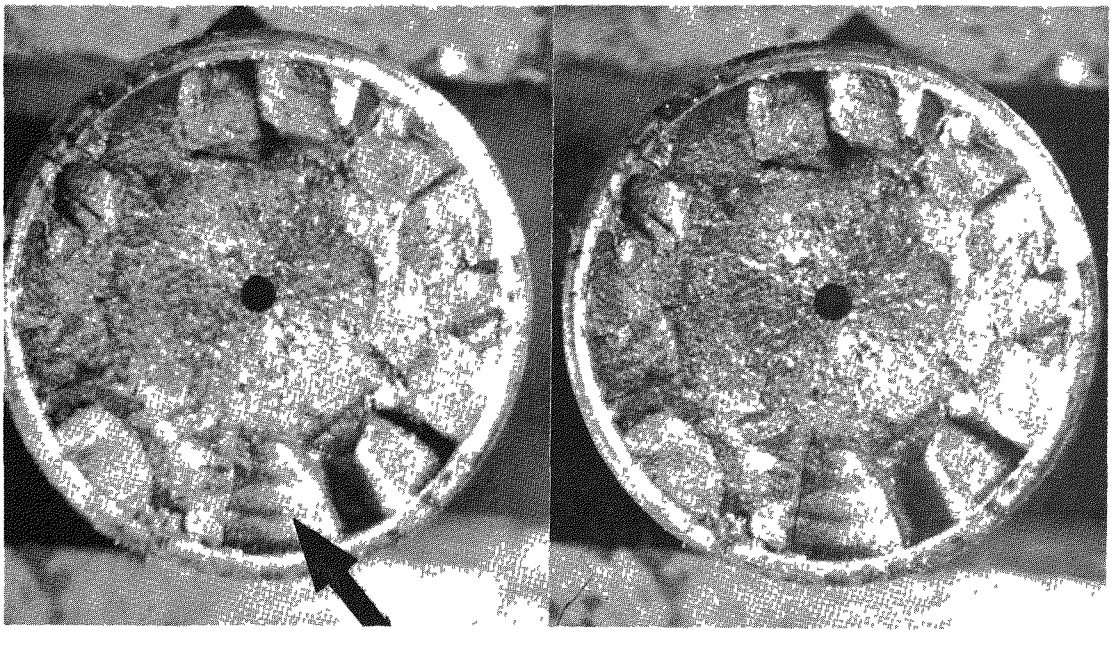

FIGURE 21 Central void surrounded by small columnar grains and dark rings in outer oxide (arrow) of Element DEH. (stereopair).
Magnification 4X. Reference No. 6261

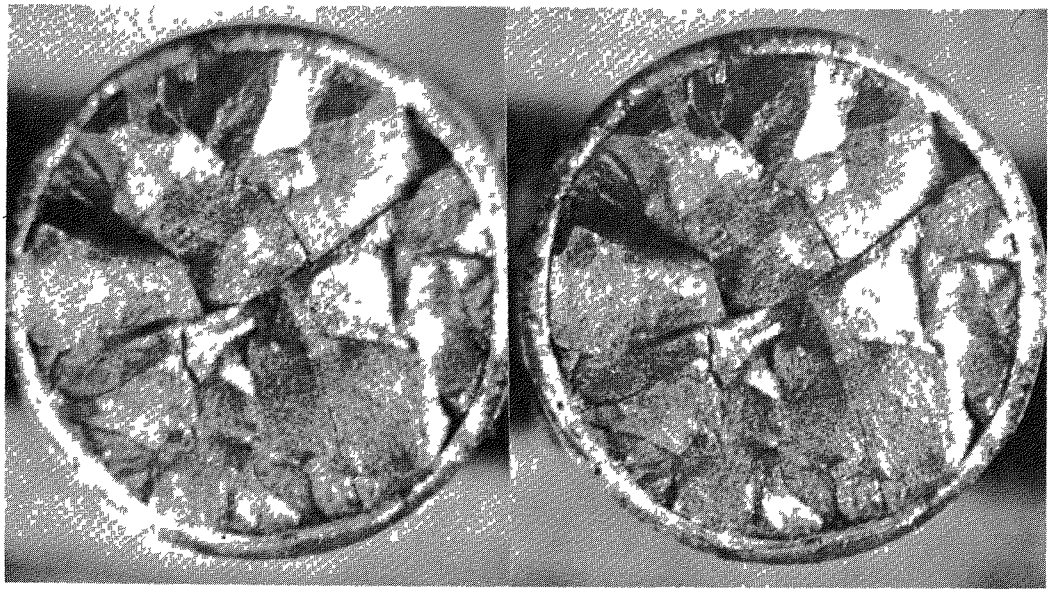

FIGURE 22 Typical UO_2 section which had not undergone grain growth. Note random cracking. Element DEF. (stereopair).
Magnification 4X. Reference No. 6341.

FIG. 23
ΔP & THERMOCOUPLE DATA